Supporting information

2,2'-Bipyrimidine based Luminescent Ru(II)/Ir(III)-Arene Monometallic, Homo and Heterobimetallic Complexes for therapy Against MDA-MB-468 and Caco-2 cell†

Nilmadhab Roy,‡ Utsav Sen,‡ Prithvi Moharana,‡ Lavanya Thilak Babu, Binoy Kar, Seshu Vardhan, Suban K Sahoo, Bipasha Bose,* Priyankar Paira*

NMR, ESI-MS, IR Spectra	**2-21**
Table S1:	**21**
Fig. S1-S3	**22-23**
Table S2	**24**
Fig. S4-S5	**25-31**
Fig. S6-S7	**32-33**
Table S3	**33**
Fig. S8	**34**
Table S4	**35**
Fig. S9-S10	**35**
Fig. S11	**36**
Experimental Section	**36-46**
References	**46-48**

NMR, ESI-MS, IR Spectra

^{1}H NMR Spectrum of complex LRu

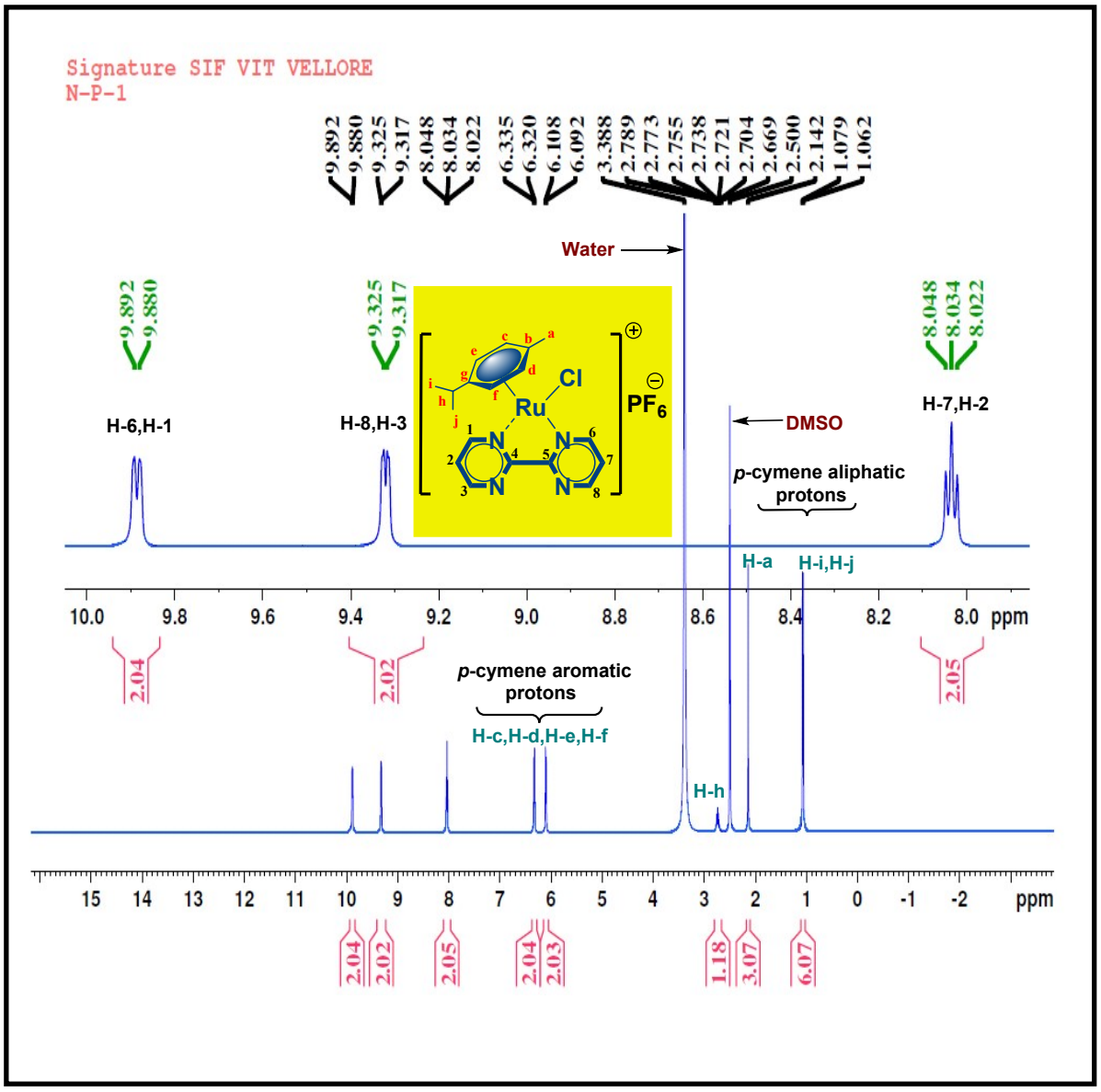

^{31}P NMR Spectrumof LRu

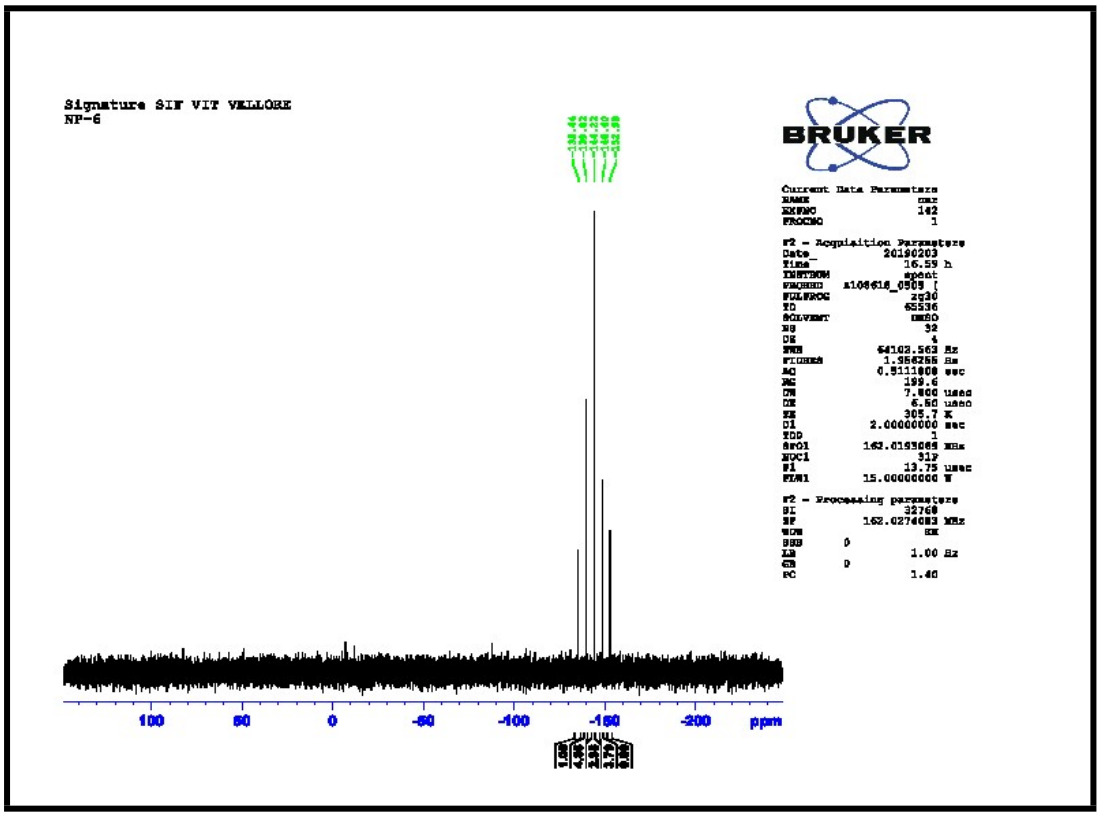

^{19}F NMR Spectrumof LRu

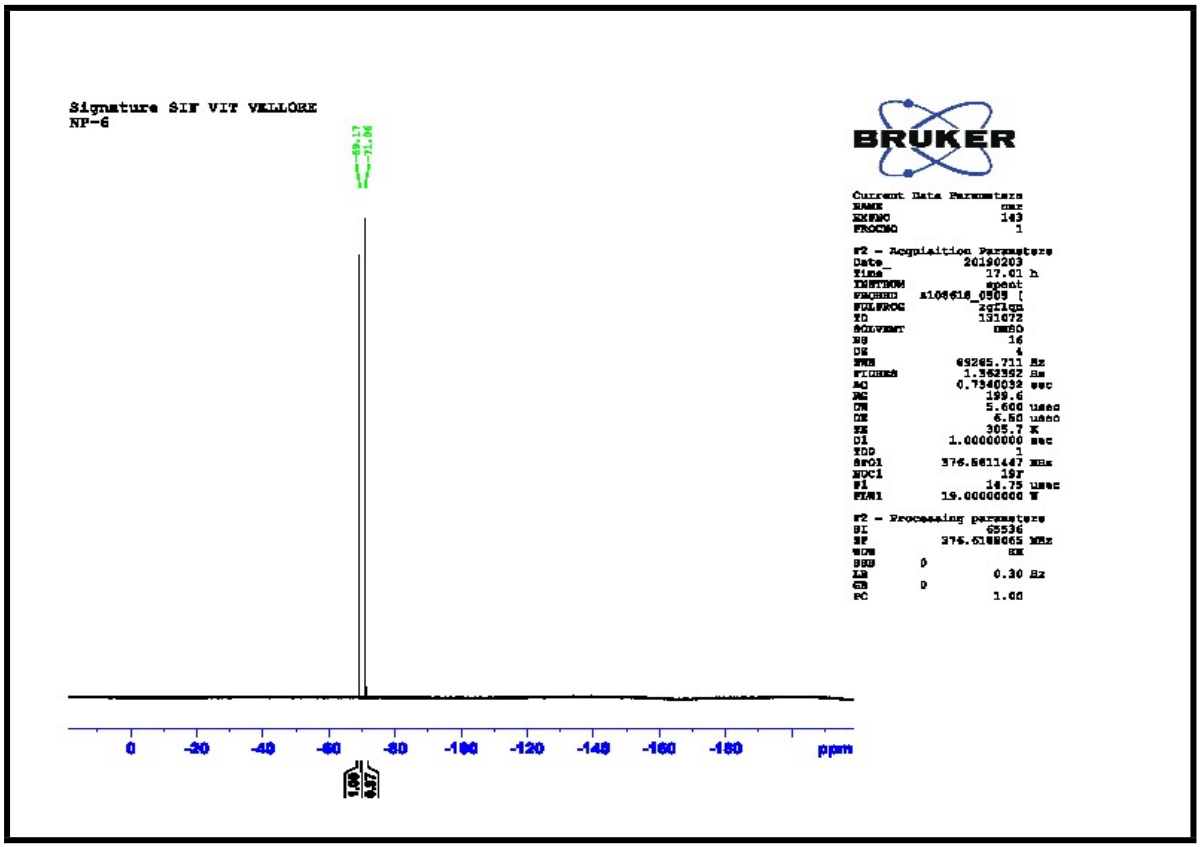

ESI-MS of LRu

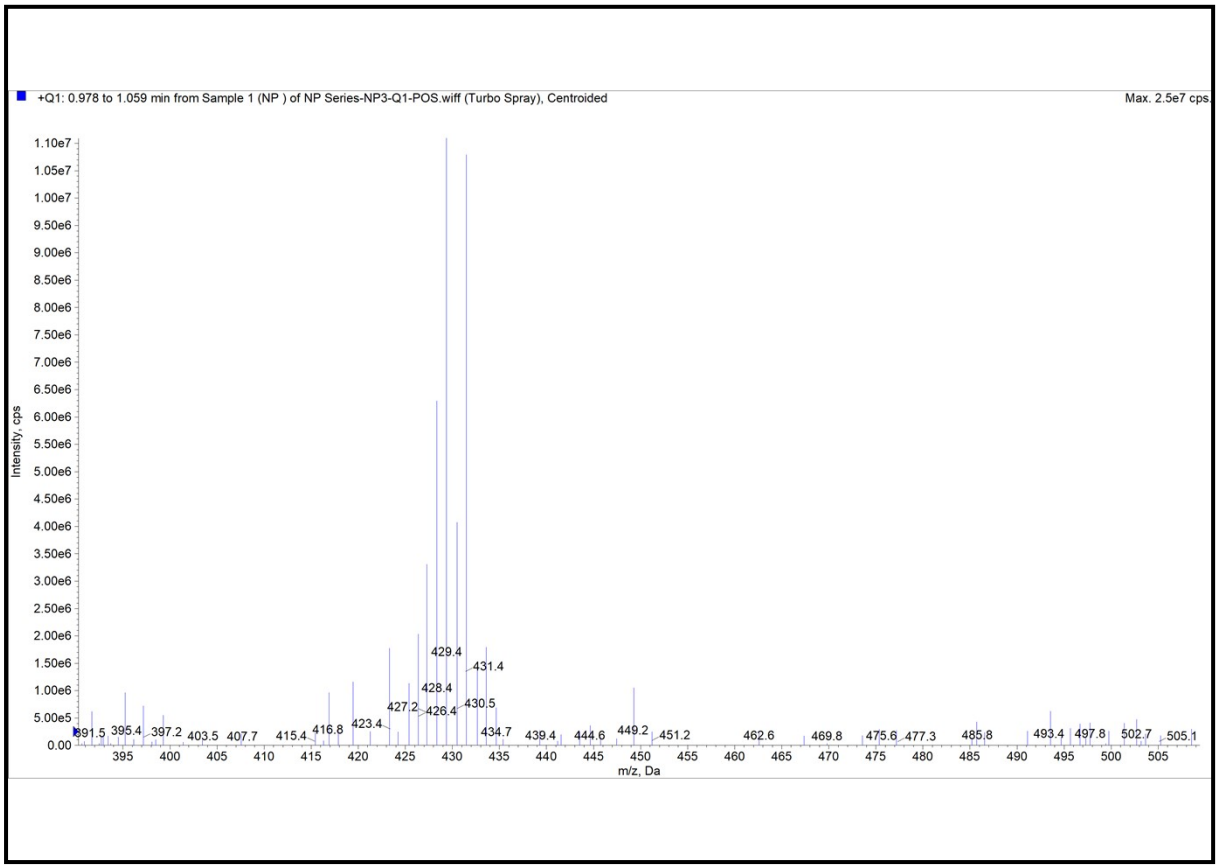

FT-IR Spectrum of LRu

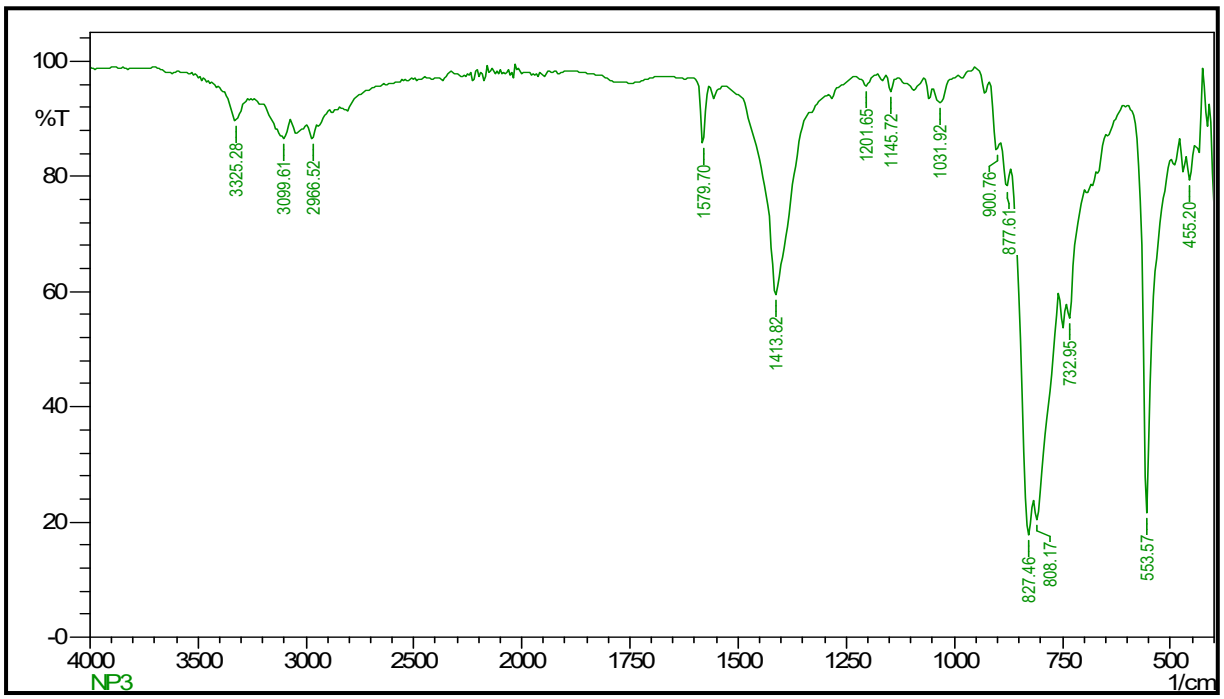

^{1}H NMR Spectrum of complex LIr

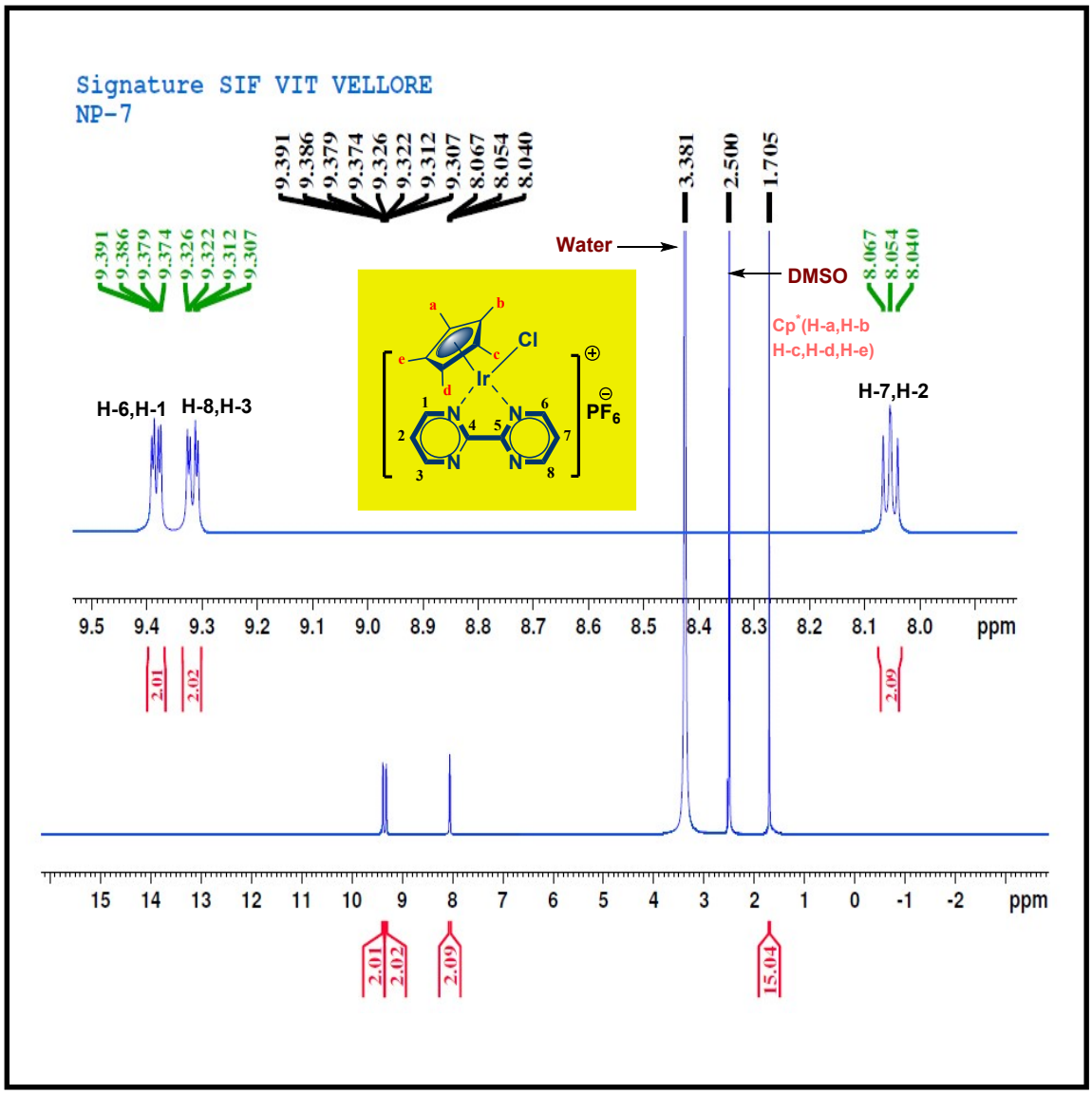

^{31}P NMR Spectrumof LIr

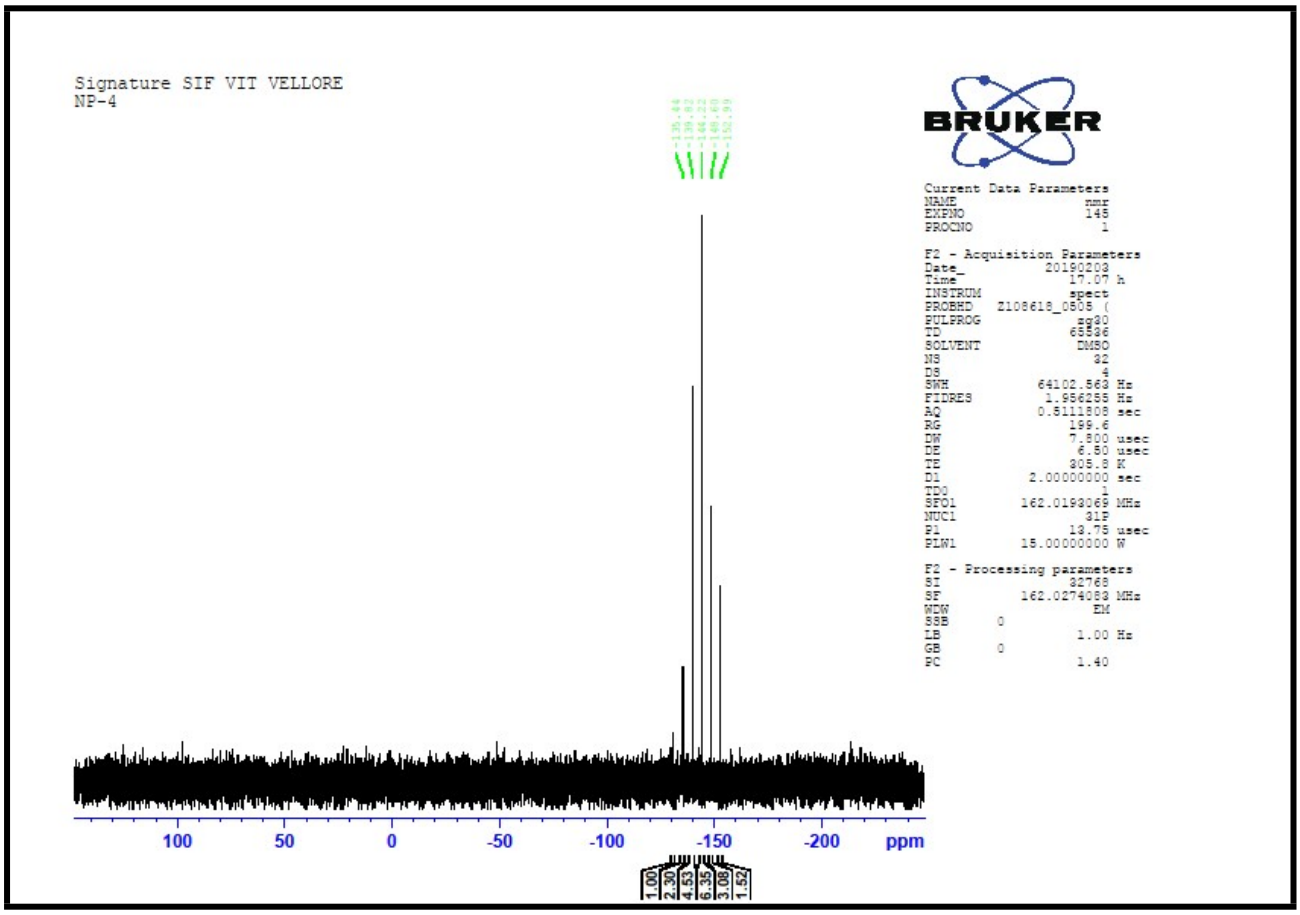

^{19}F NMR Spectrumof LIr

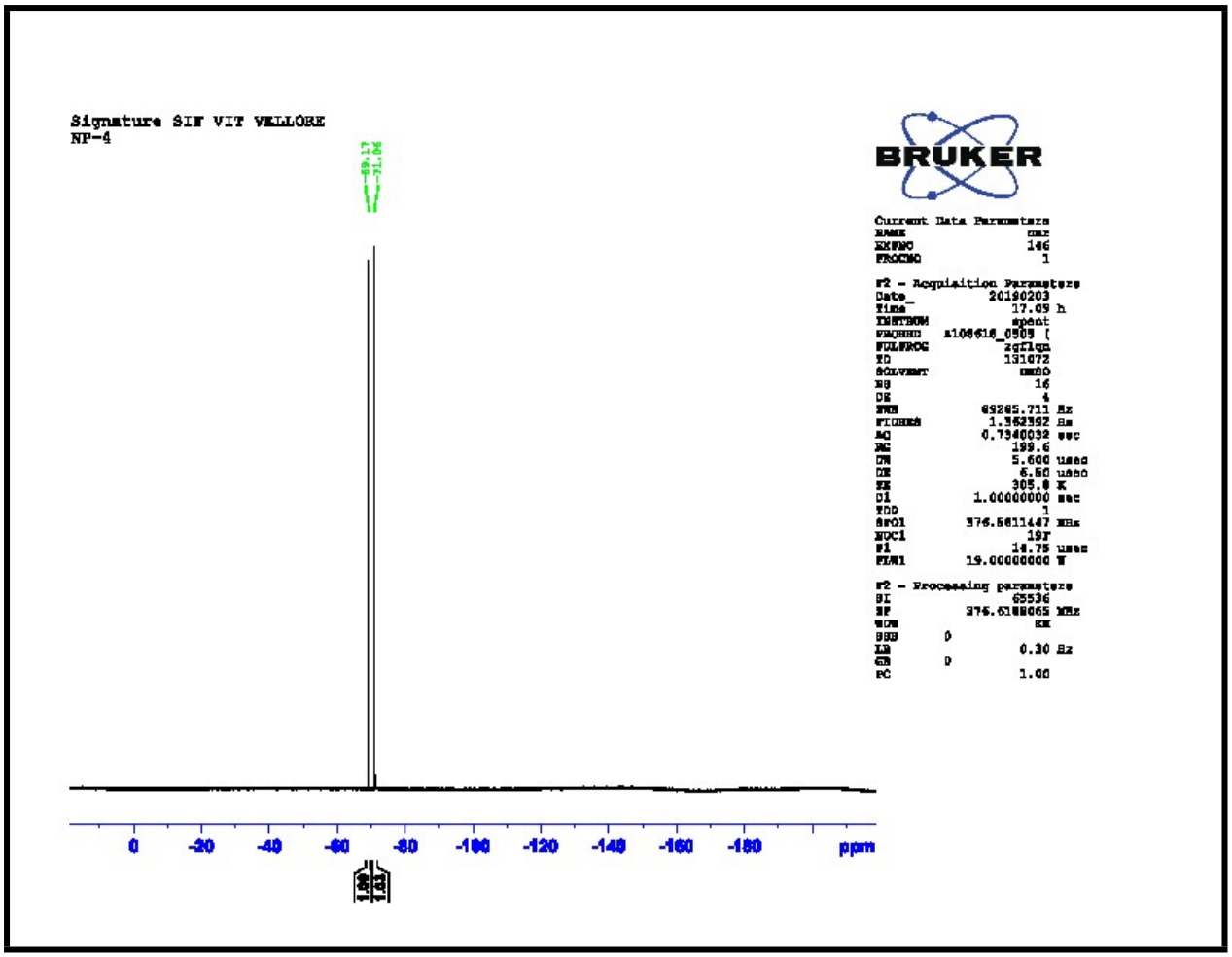

ESI-MS of LIr

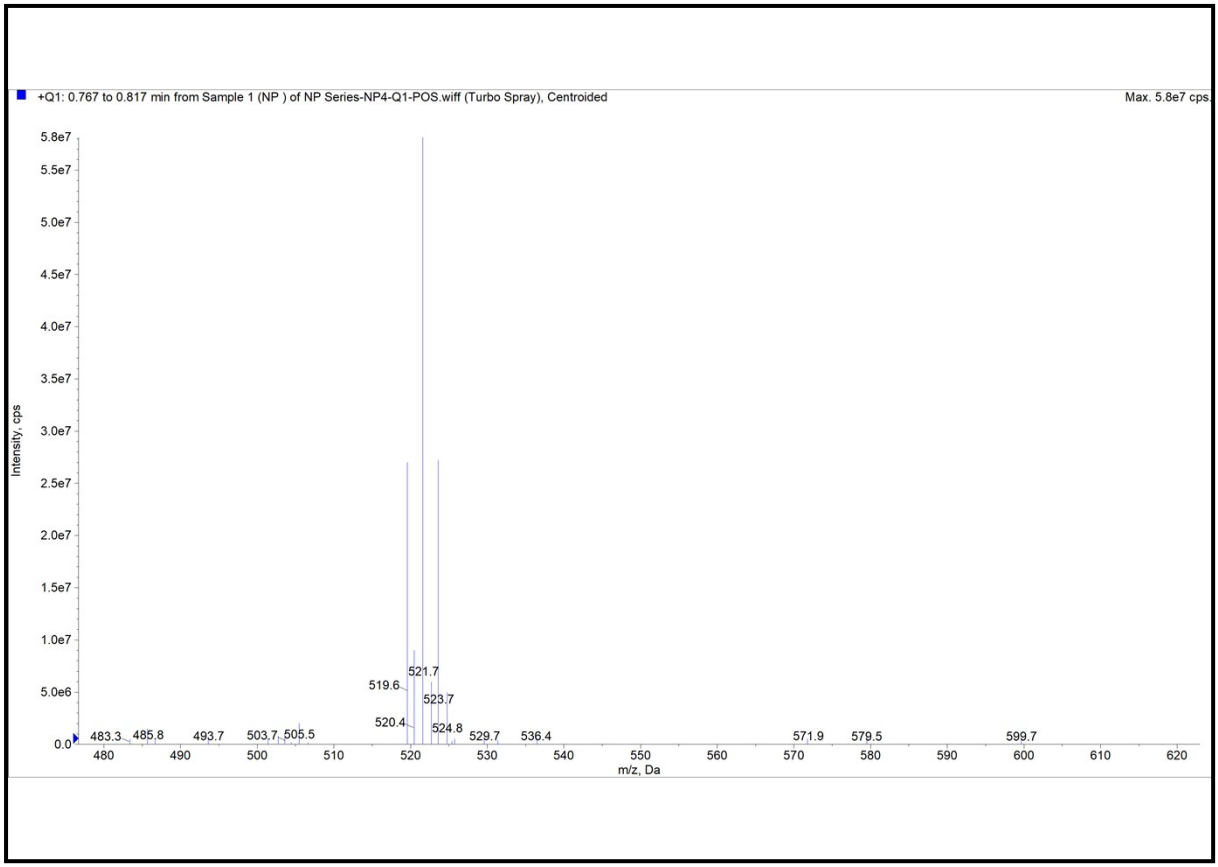

FT-IR Spectrum of LIr

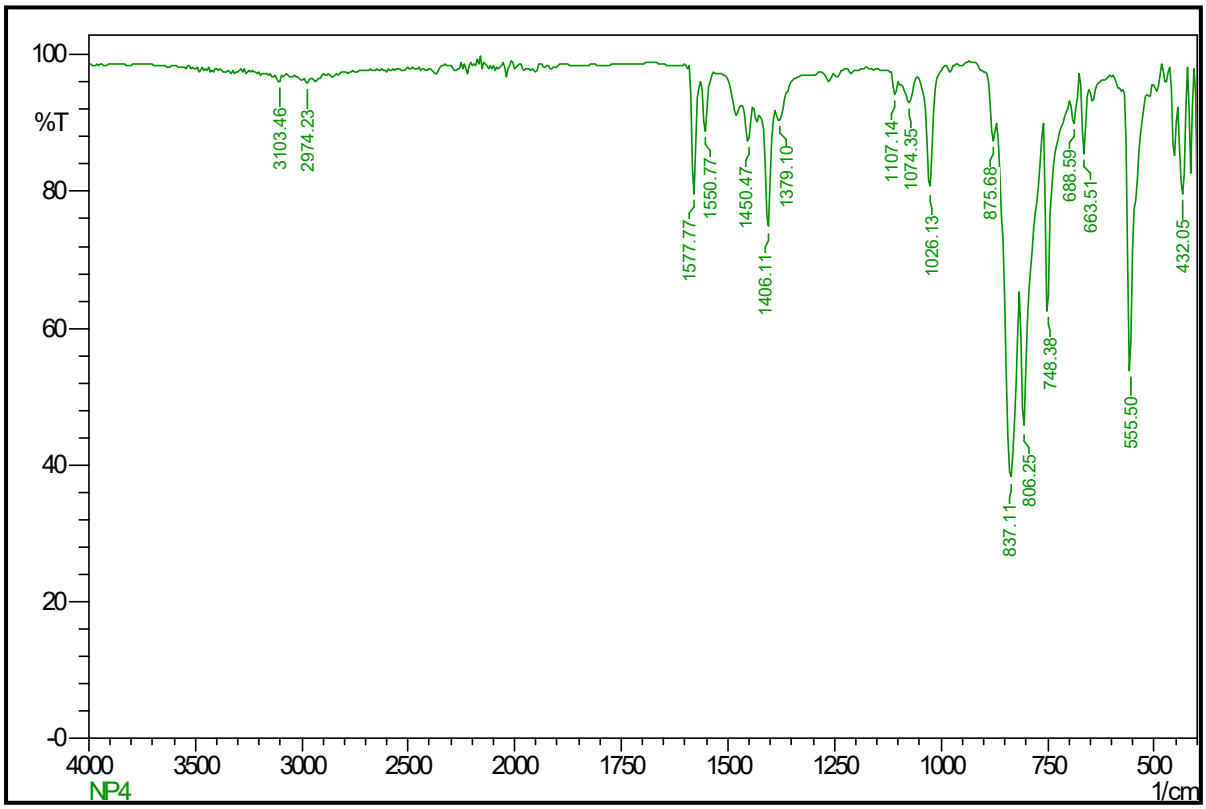

^{1}H NMR Spectrum of complex LRu_2

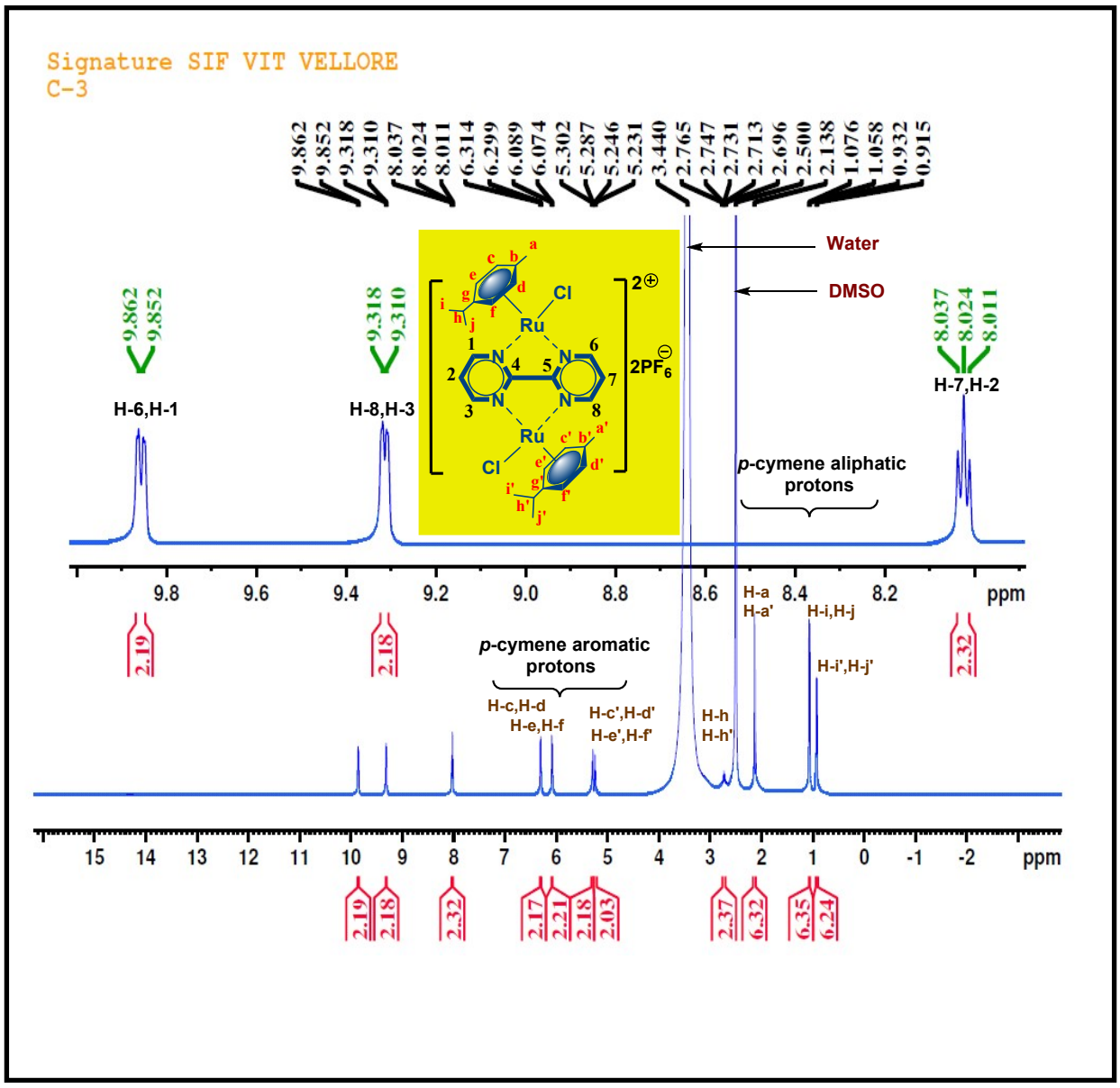

^{31}P NMR Spectrumof LRu_2

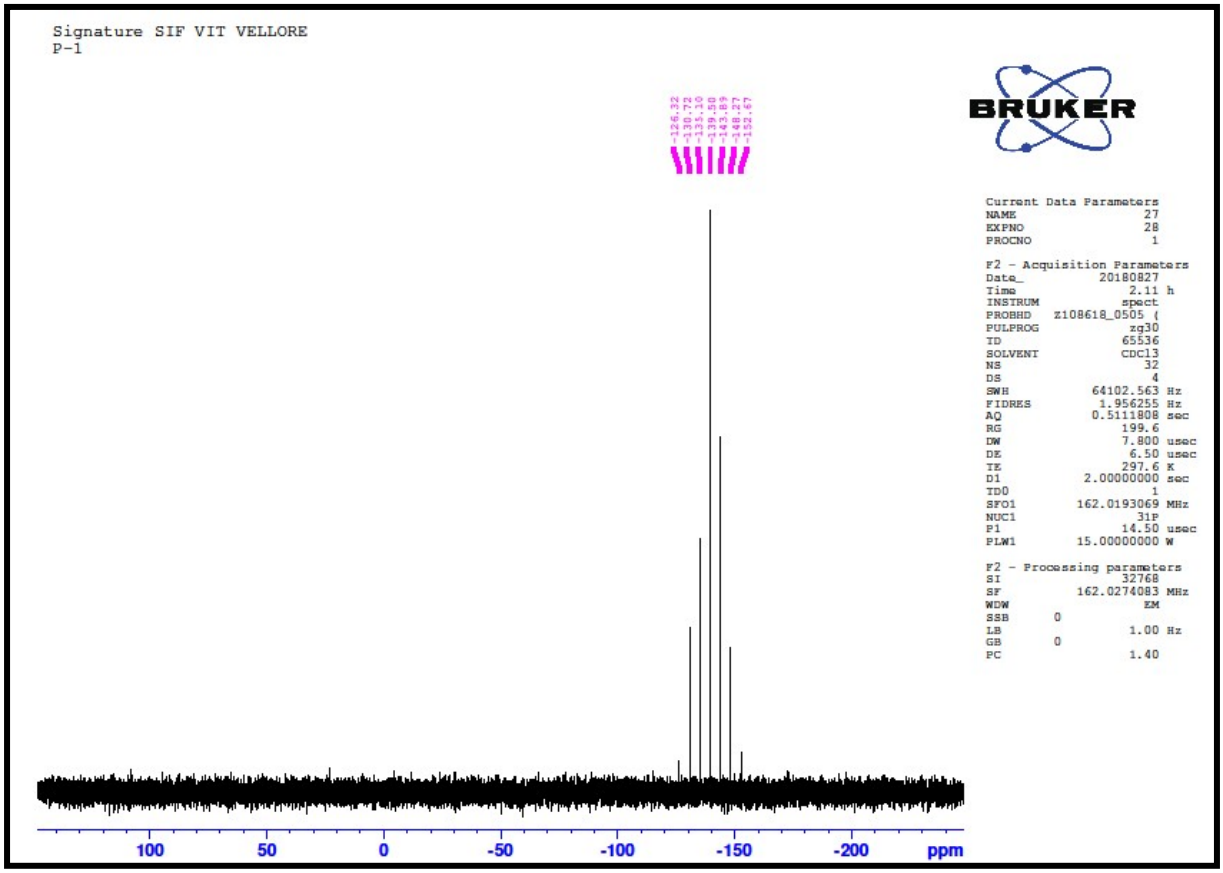

^{19}F NMR Spectrum of LRu_2

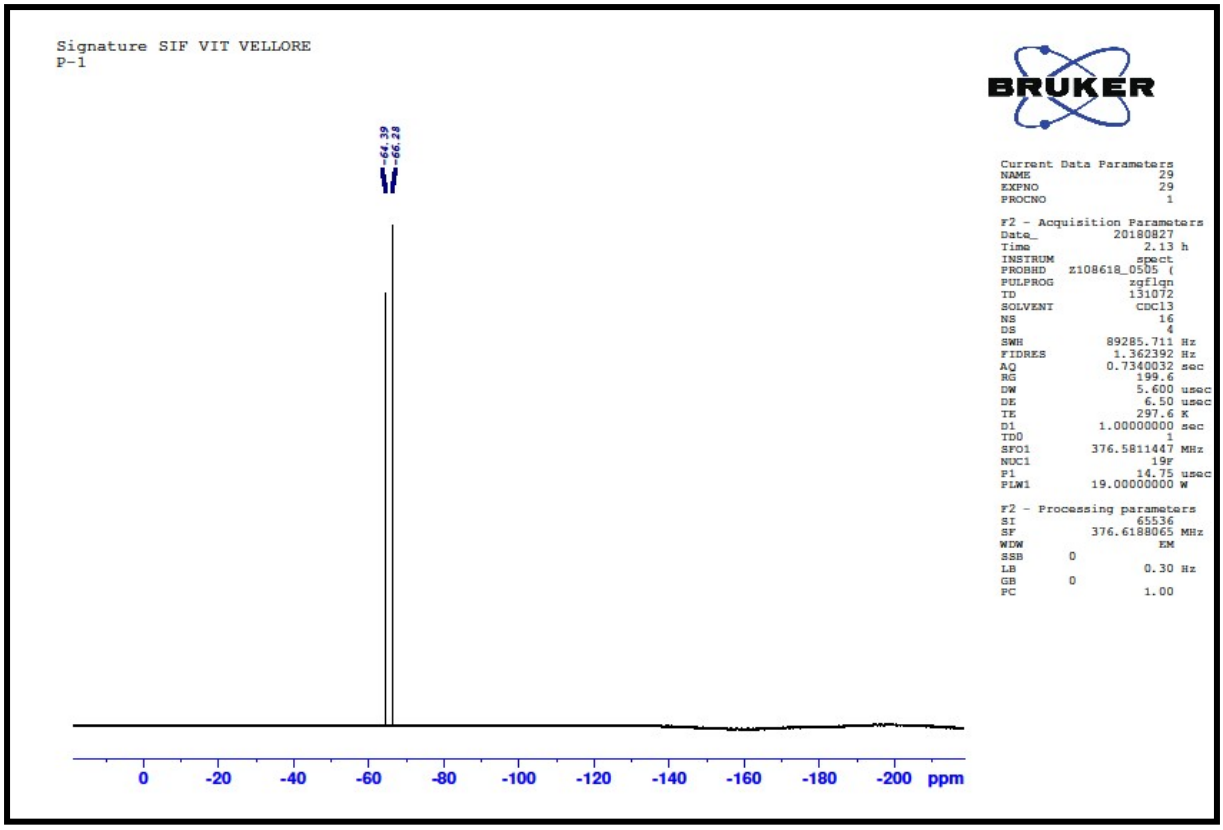

ESI-MS of LRu_2

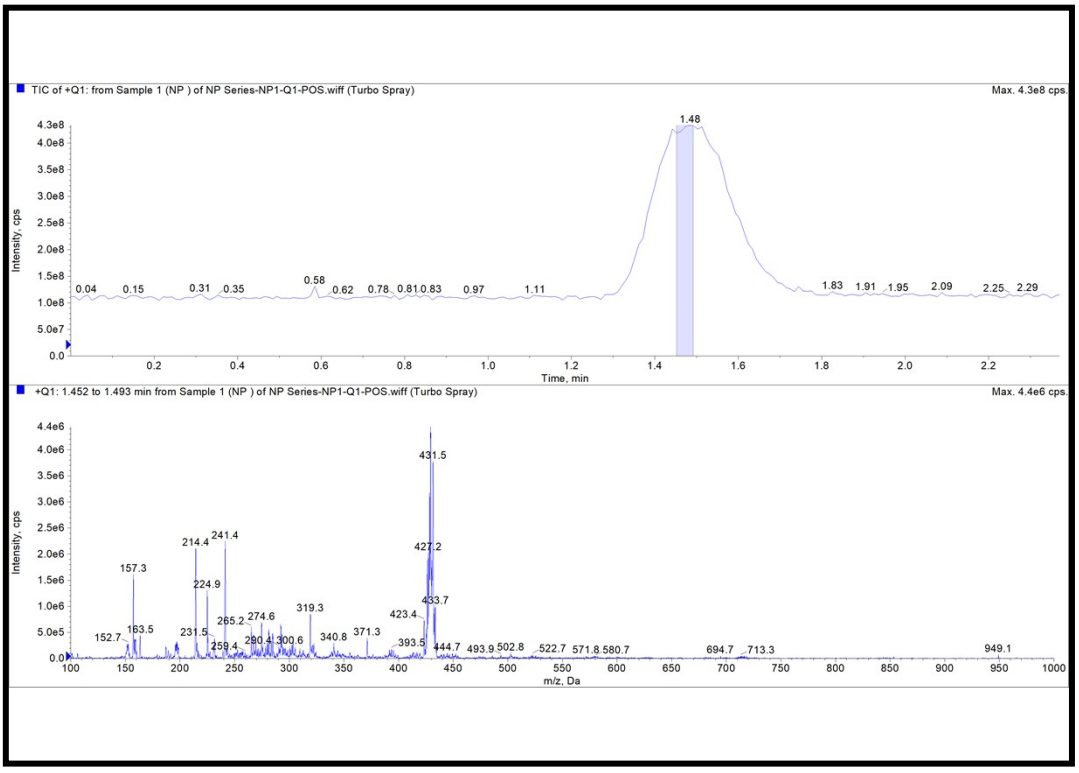

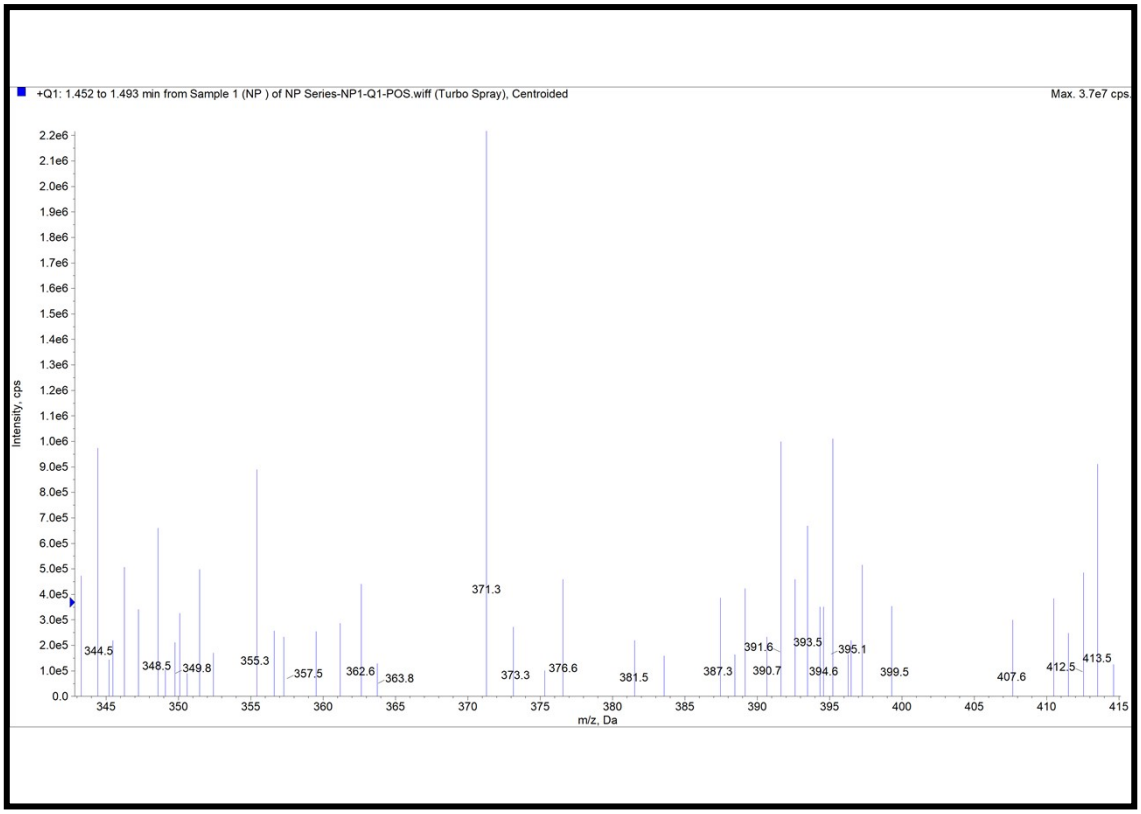

FT-IR Spectrum of LRu_2

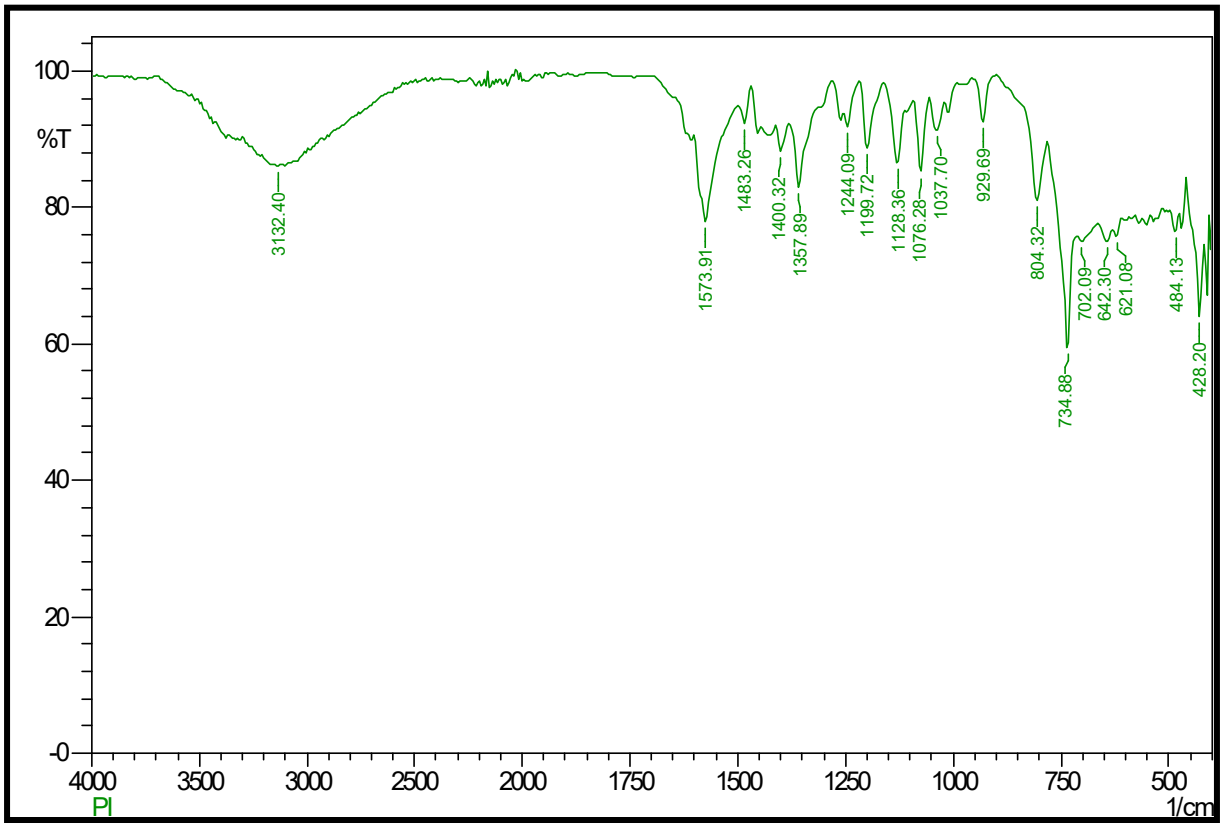

^{1}H NMR Spectrum of complex LIr_2

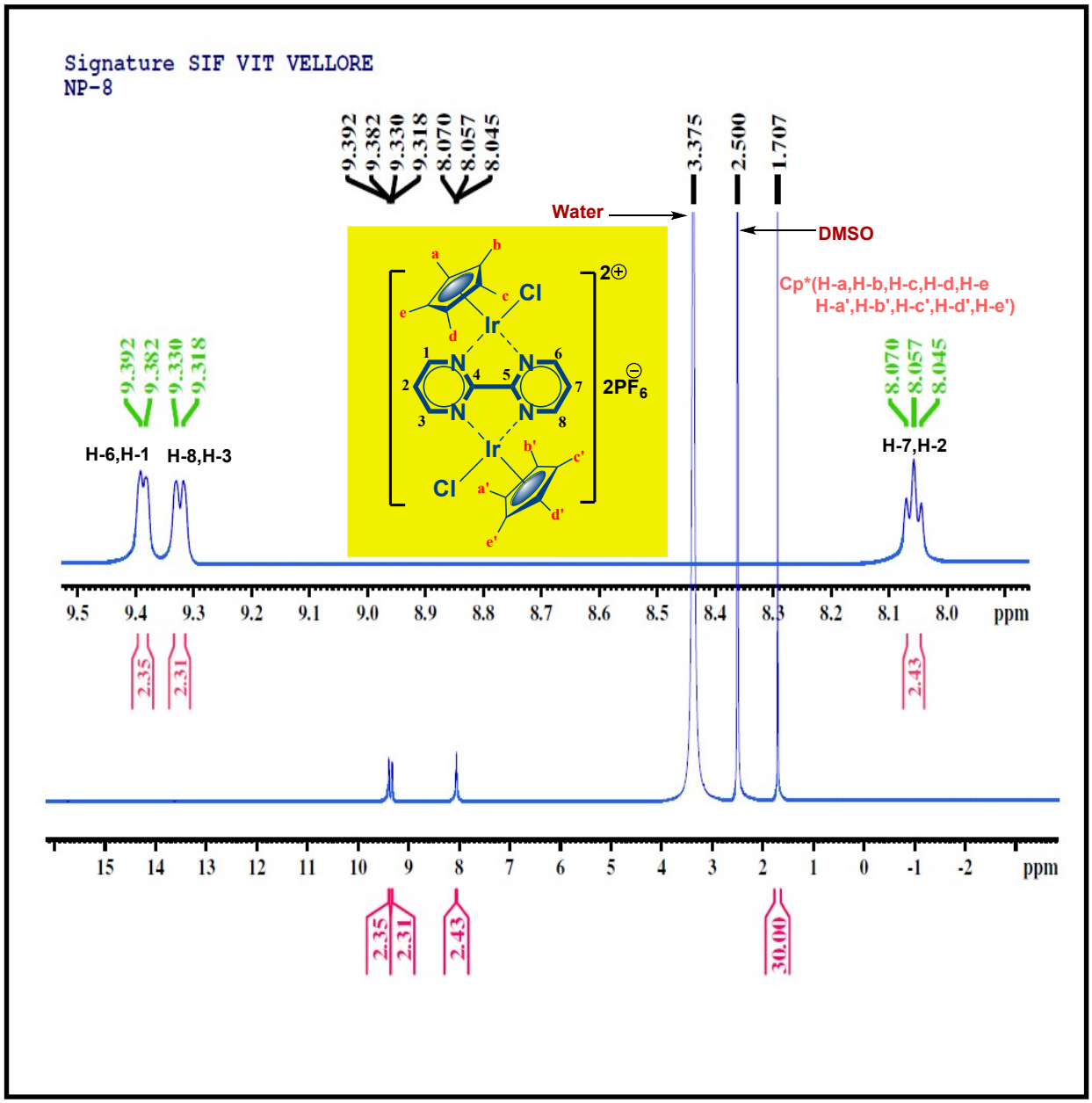

^{31}P NMR Spectrum of LIr_2

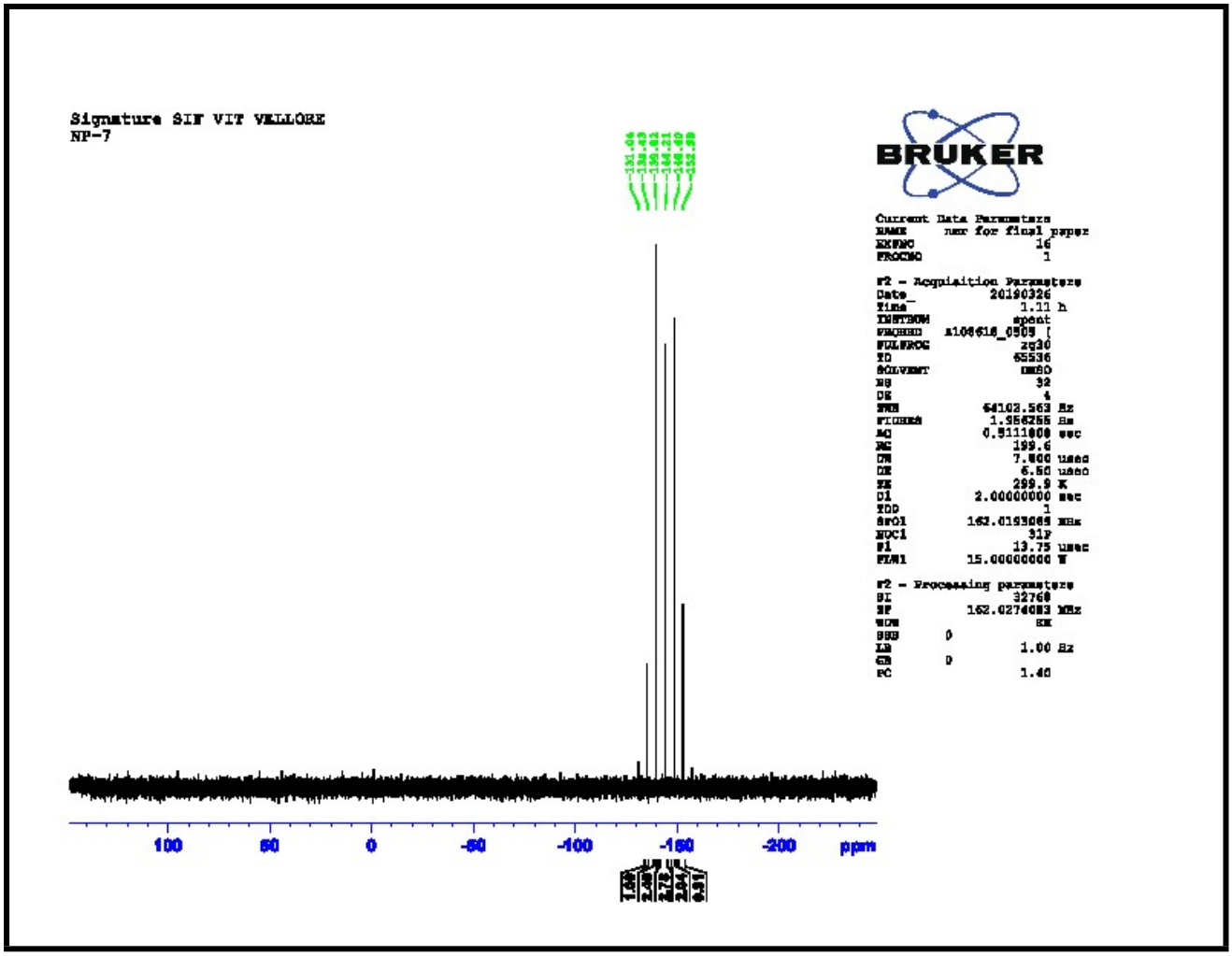

^{19}F NMR Spectrum of LIr_2

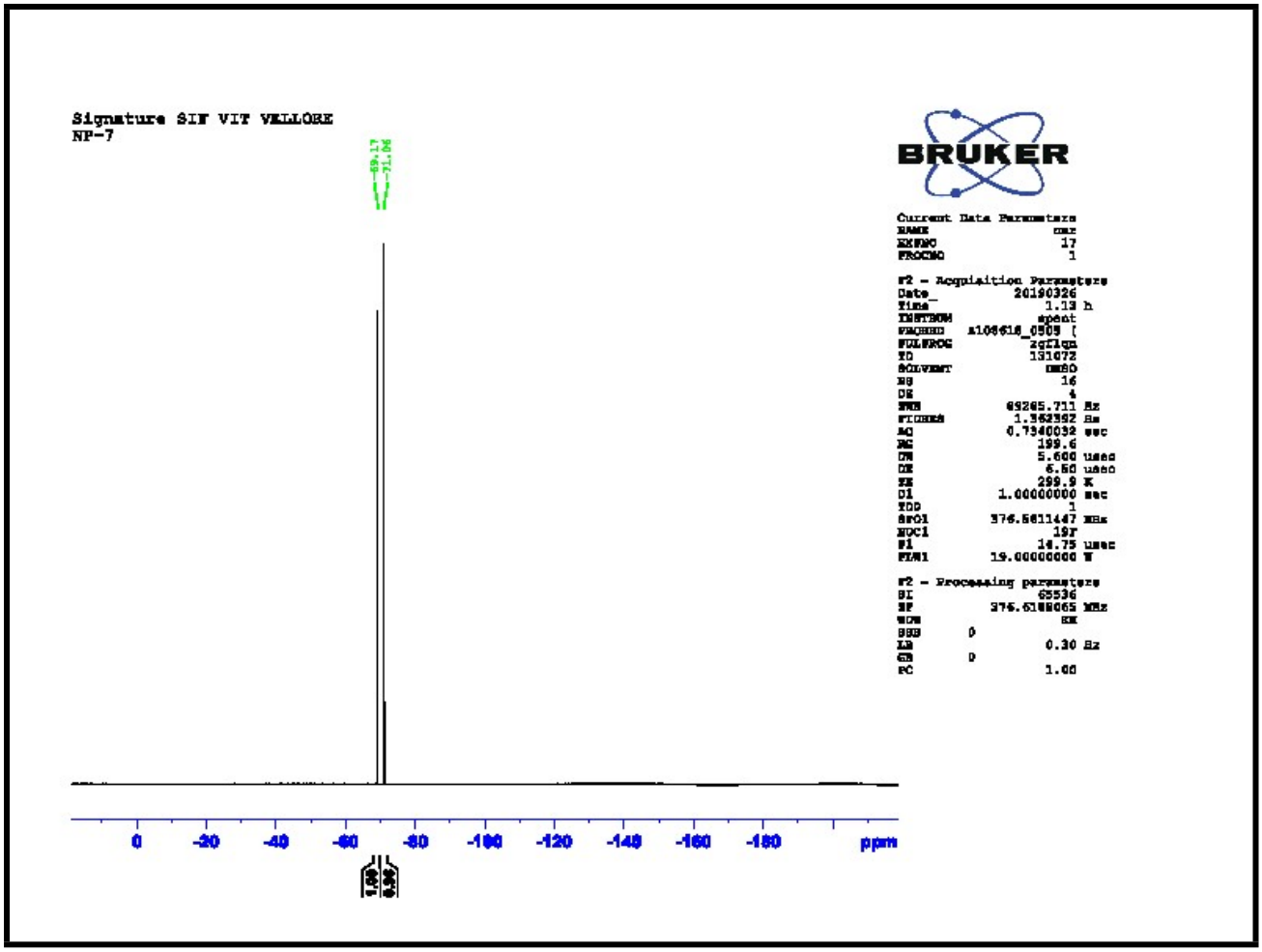

ESI-MS of LIr_2

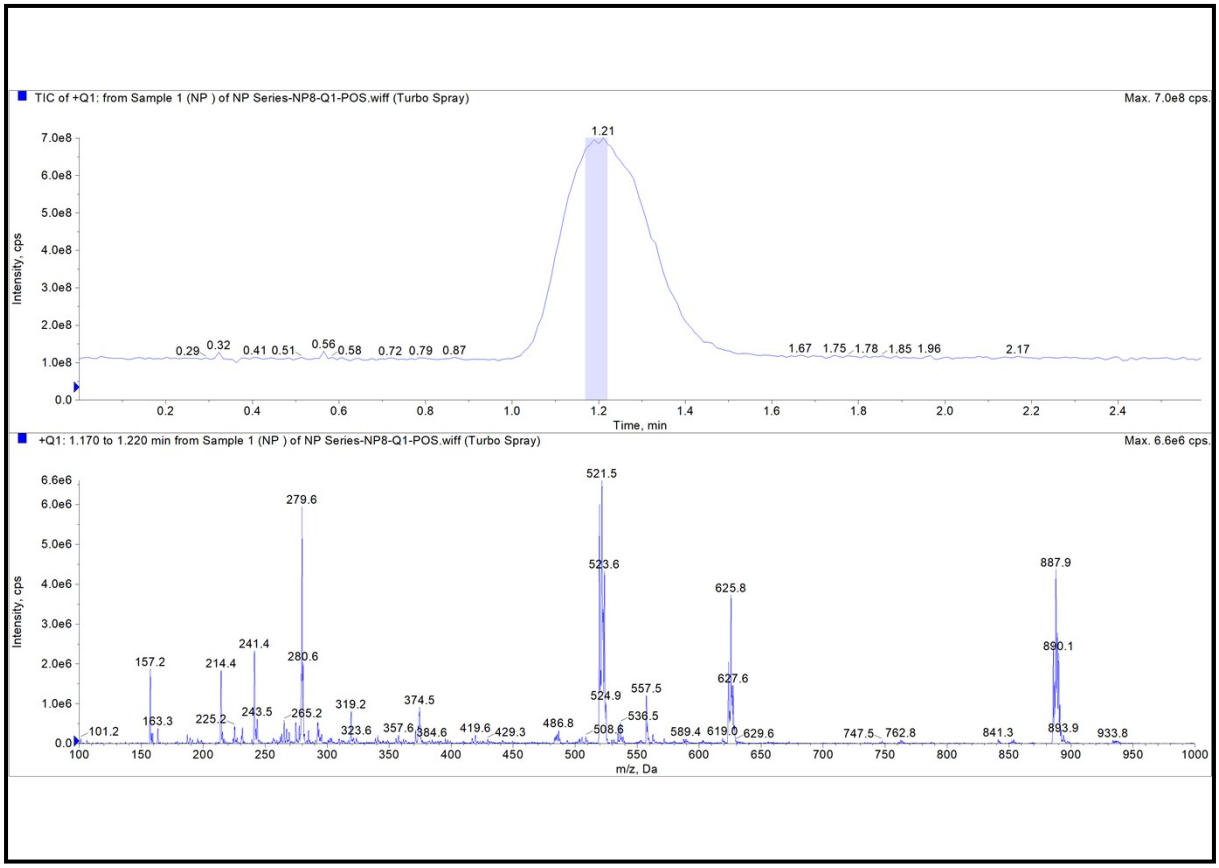

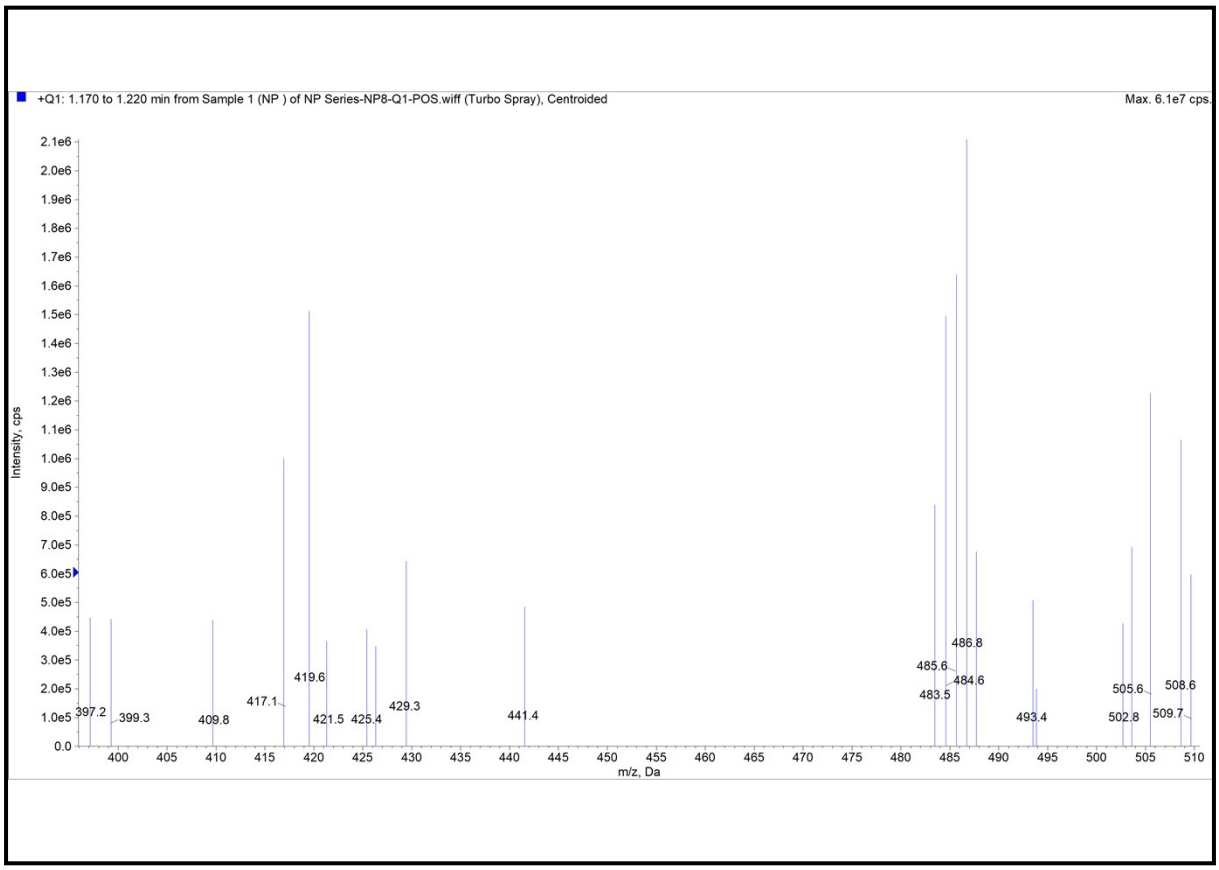

FT-IR Spectrum of LIr_2

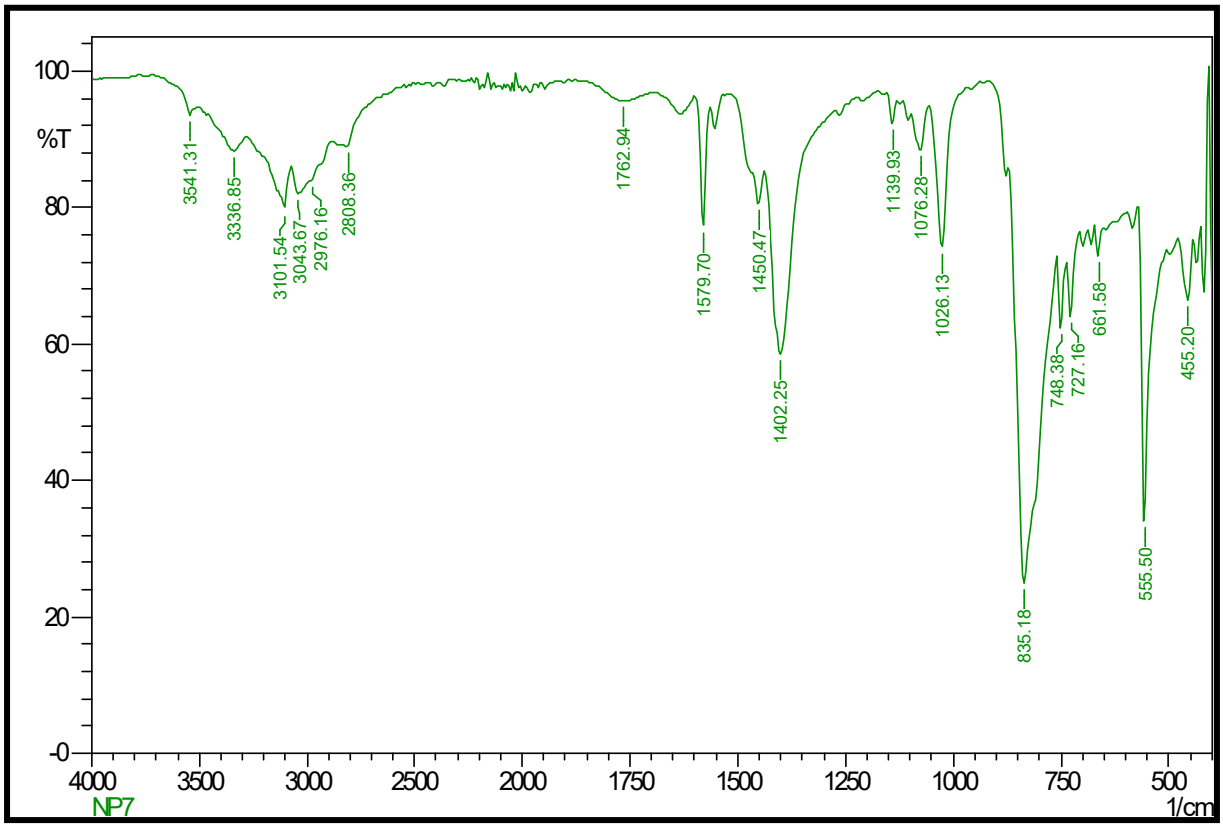

^{1}H NMR Spectrum of complex LRuIr

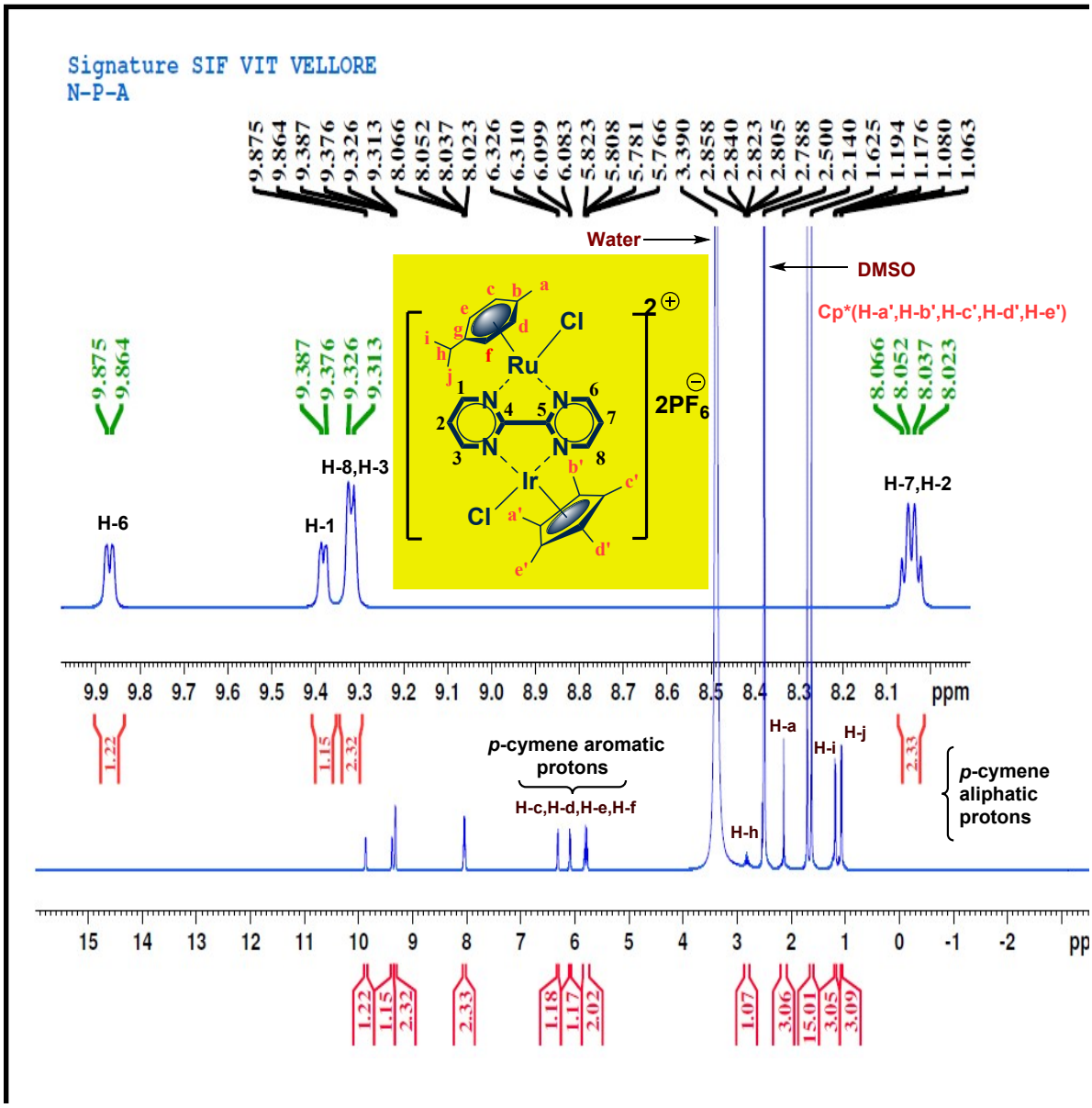

^{31}P NMR Spectrum of LRuIr

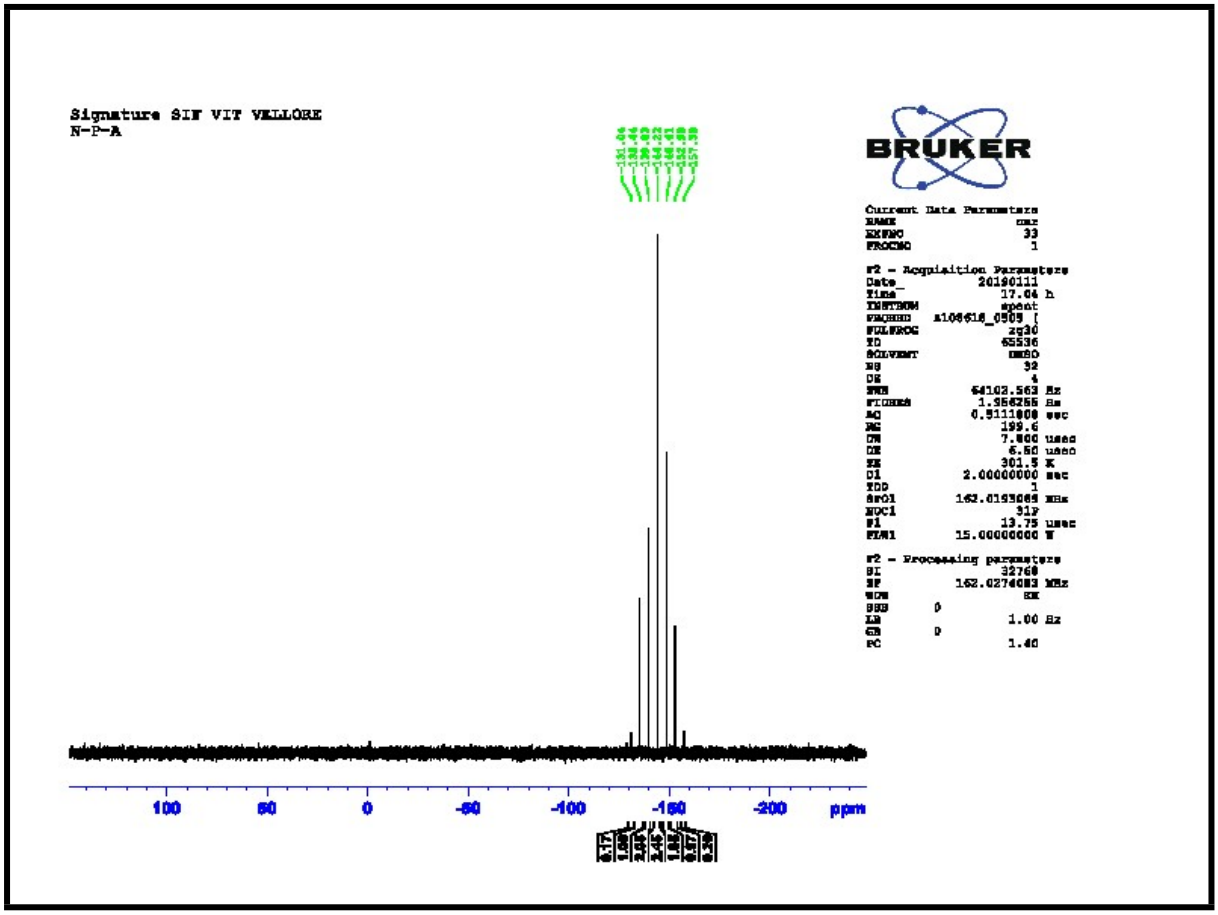

^{19}F NMR Spectrum of LRuIr

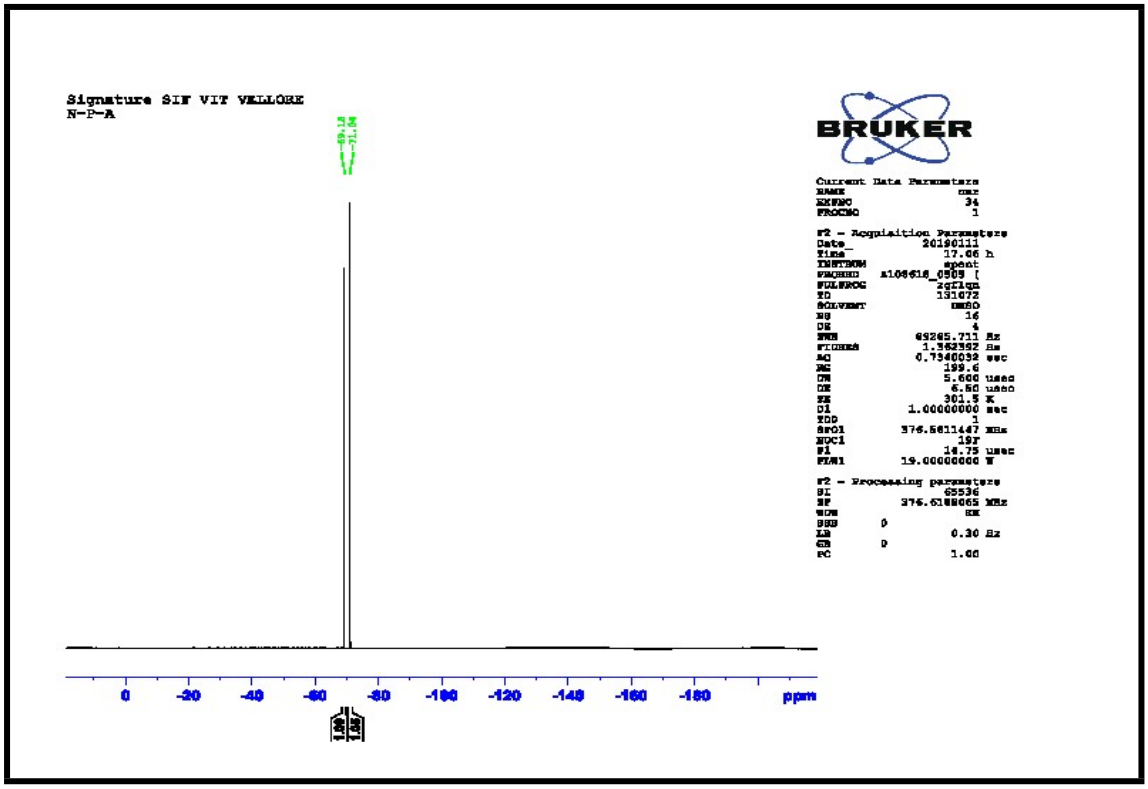

ESI-MS of LRuIr

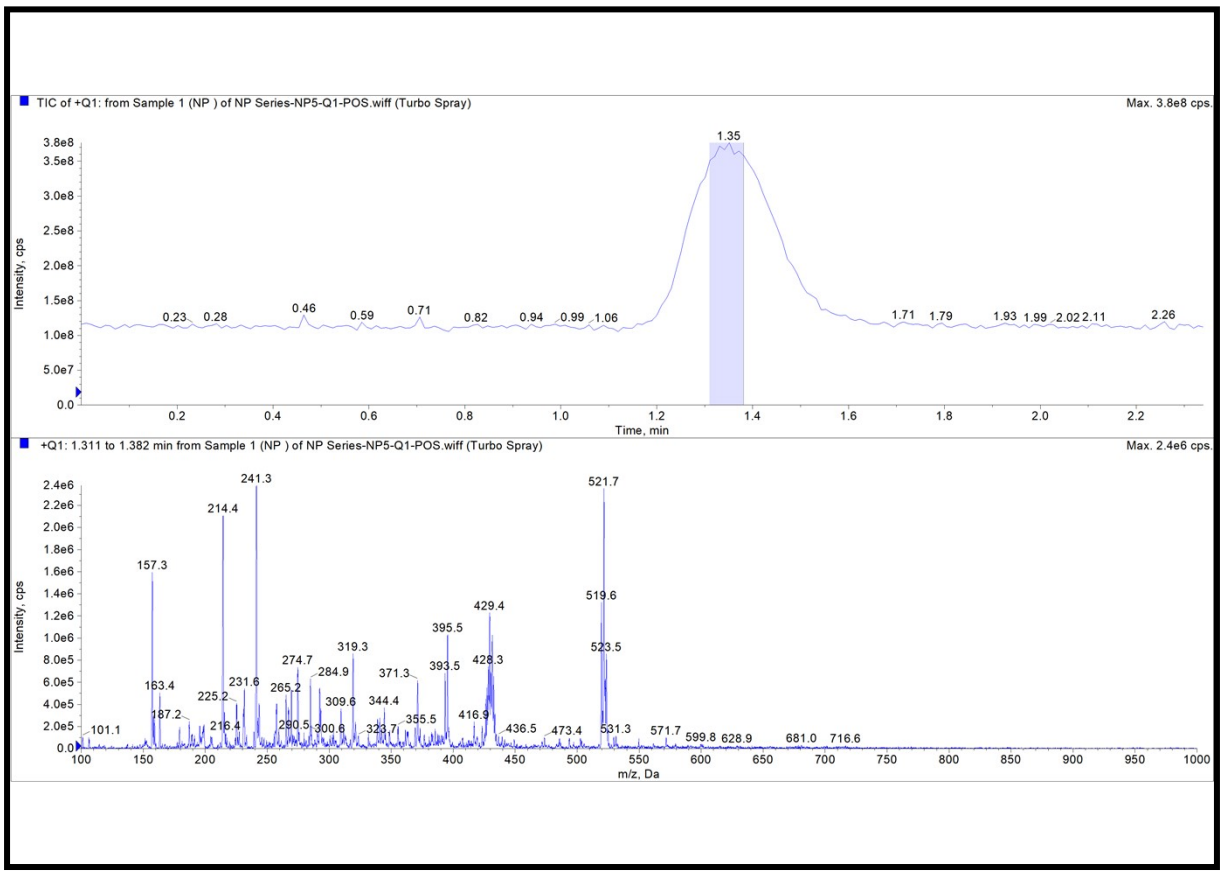

FT-IR Spectrum of LRuIr

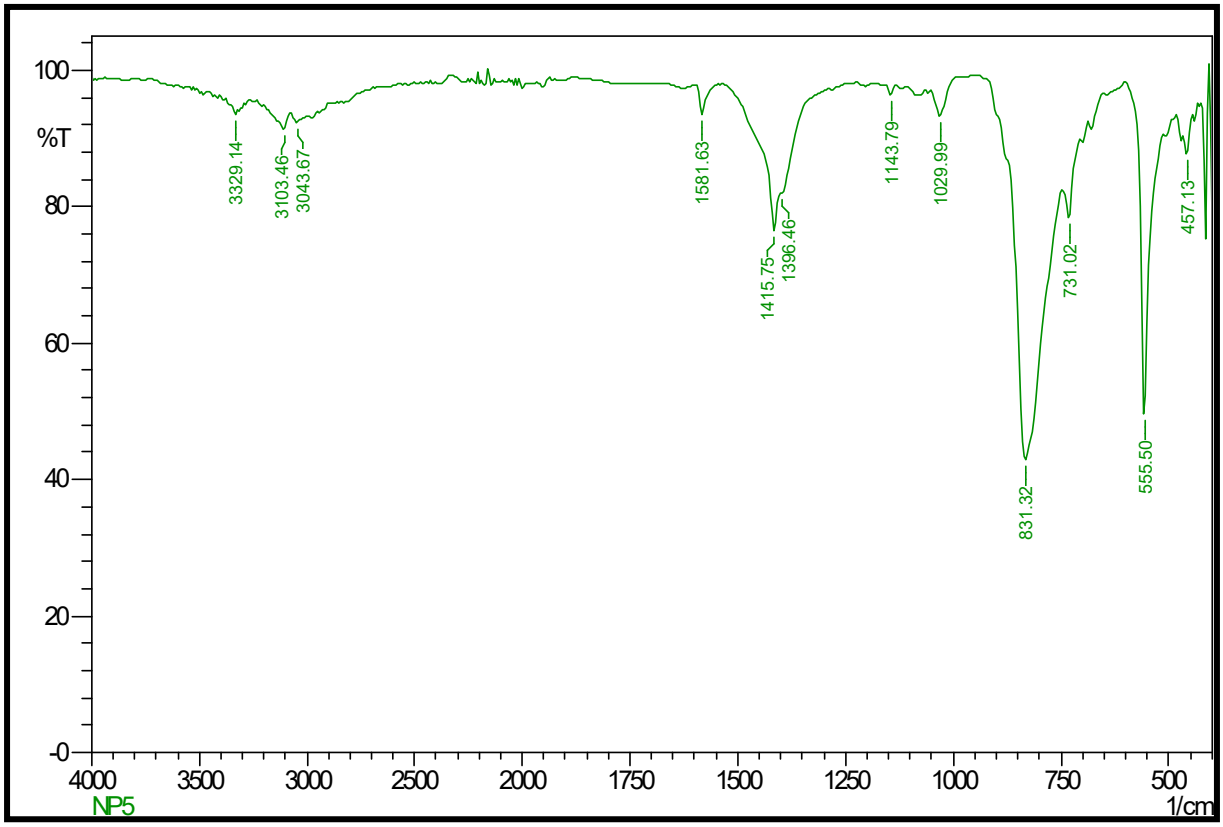

Table S1: Photophysical characterization, solubility, lipophilicity and conductivity

Samples	λmax (nm)[a]	λ_f (nm)[b]	Stoke's shift	ε (M^{-1} cm^{-1})[c]	(φ_f)[d]	solubility (M)[e]	log P[f]	Λ_M[g] (µs) DMSO	10% DMSO
LRu	400	500	100	4000	0.08	0.028	0.98±0.14	19	72
LRu_2	400	500	100	7333	0.12	0.034	1.39±0.09	21	240
LIr	380	500	120	3333	0.09	0.030	1.31±0.08	22	81
LIr_2	380	500	120	5000	0.18	0.037	1.60±0.27	24	290
LRuIr	400	500	100	7666	0.19	0.040	1.62±0.13	25	295
Quinine Sulphate	350	450	100	-	0.541	-	-	-	

[a]absorption maxima, [b]maximum emission wavelength, [c]extinction coefficient, [d]quantum yield, [e]DMSO-10% DMEM medium (1:99 v/v, comparable to cell media), [f]n-octanol/aqueous phosphate buffer partition coefficient in presence of 130 mM NaCl, [g]conductance in DMSO and 10% aqueous DMSO (complex concentration 3 x 10^{-5} M)

UV & Fluorescence Spectra

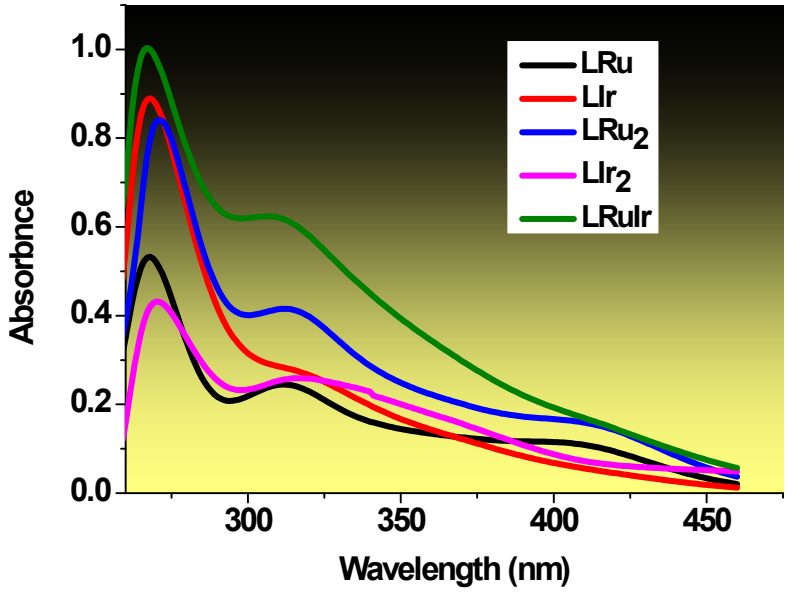

Fig. S1: UV-Vis Spectra of the complexes in DMSO: H_2O (1:9)

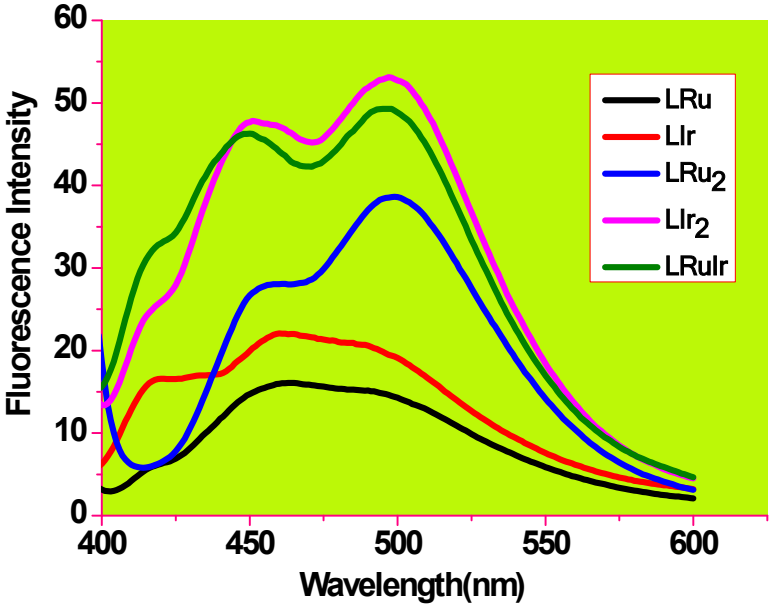

Fig. S2: Fluorescence Spectra of the complexes in DMSO: H_2O (1:9)

Stability Study

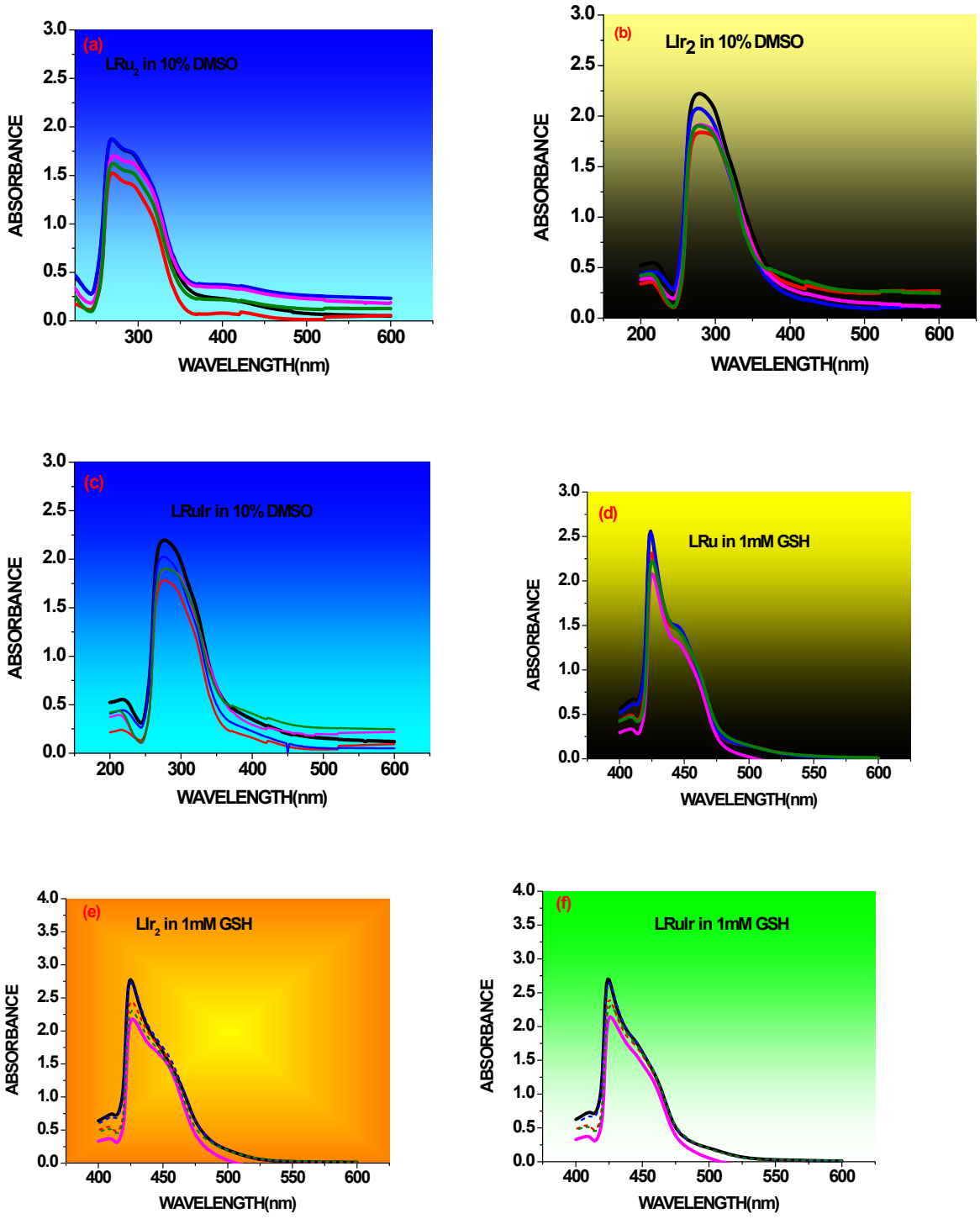

Fig. S3 Stability study of complexes (a) [LRu_2], (b) [LIr_2] and (c) [LRuIr] in 10% DMSO; (d) [LRu_2] (e) [LIr_2] and (f) [LRuIr] in 1 mM GSH medium (GSH dissolved in PBS buffer, PH 7.4)

Table S2. Molecular docking estimated free energy of binding (kcal/mol) and the inhibition constant (Ki) of the complexes with the BSA and DNA.

	Free Energy of Binding (kcal/mole)				
	[LRu]	**[LIr]**	**[LRu_2]**	**[LIrRu]**	**[LIr_2]**
BSA	-4.62	-4.72	-5.85	-5.71	-5.14
DNA	-5.72	-5.07	-7.08	-6.39	-6.06
	Inhibition Constant (Ki)				
	[LRu]	**[LIr]**	**[LRu_2]**	**[LIrRu]**	**[LIr_2]**
BSA	411.93μM	344.05μM	51.69μM	64.80μM	170.60μM
DNA	64.25 μM	191.58μM	6.94 μM	20.78μM	36.07 μM

(a)

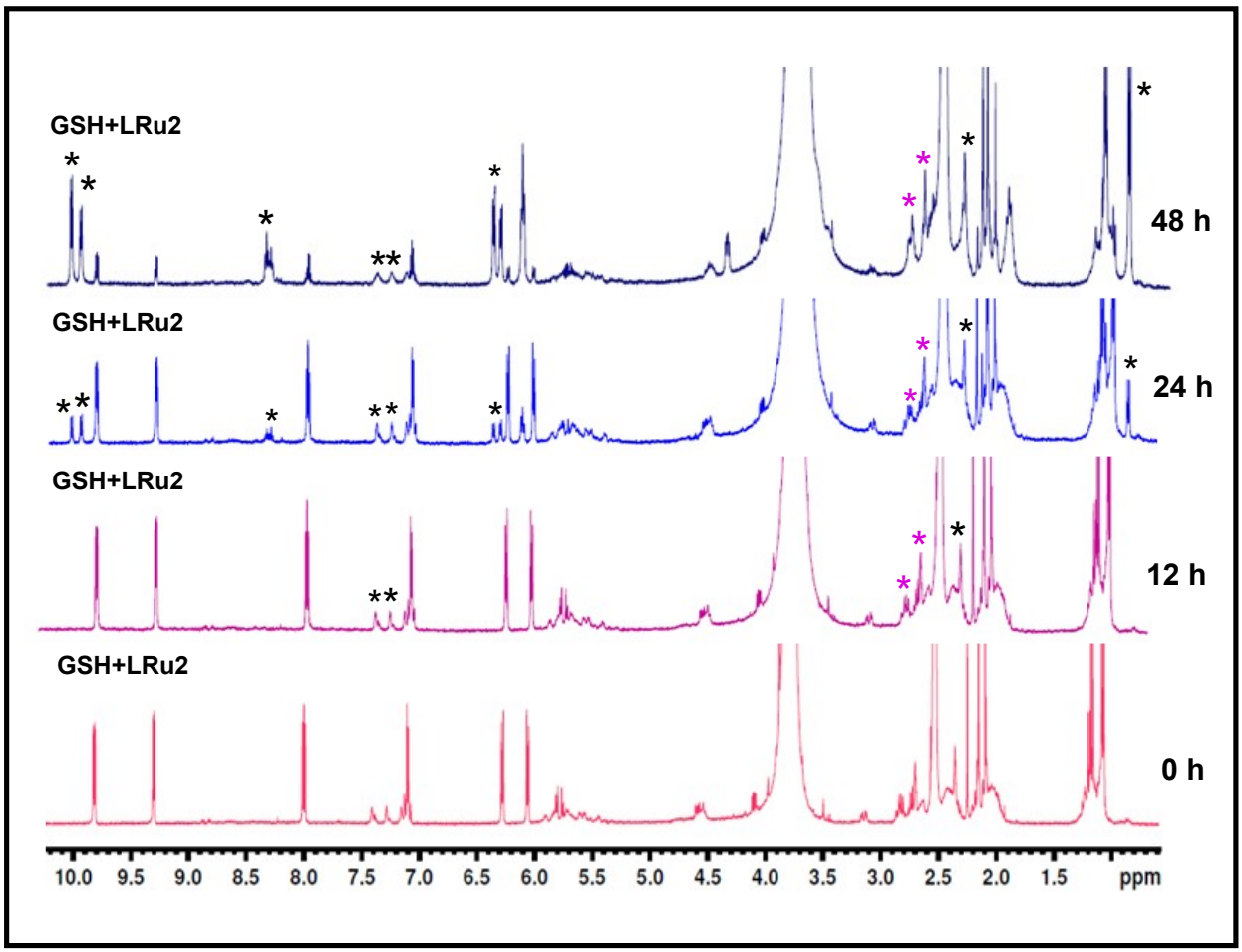
GSH+LRu2
48 h
GSH+LRu2
24 h
GSH+LRu2
12 h
GSH+LRu2
0 h
10.0 9.5 9.0 8.5 8.0 7.5 7.0 6.5 6.0 5.5 5.0 4.5 4.0 3.5 3.0 2.5 2.0 1.5 ppm

(b)

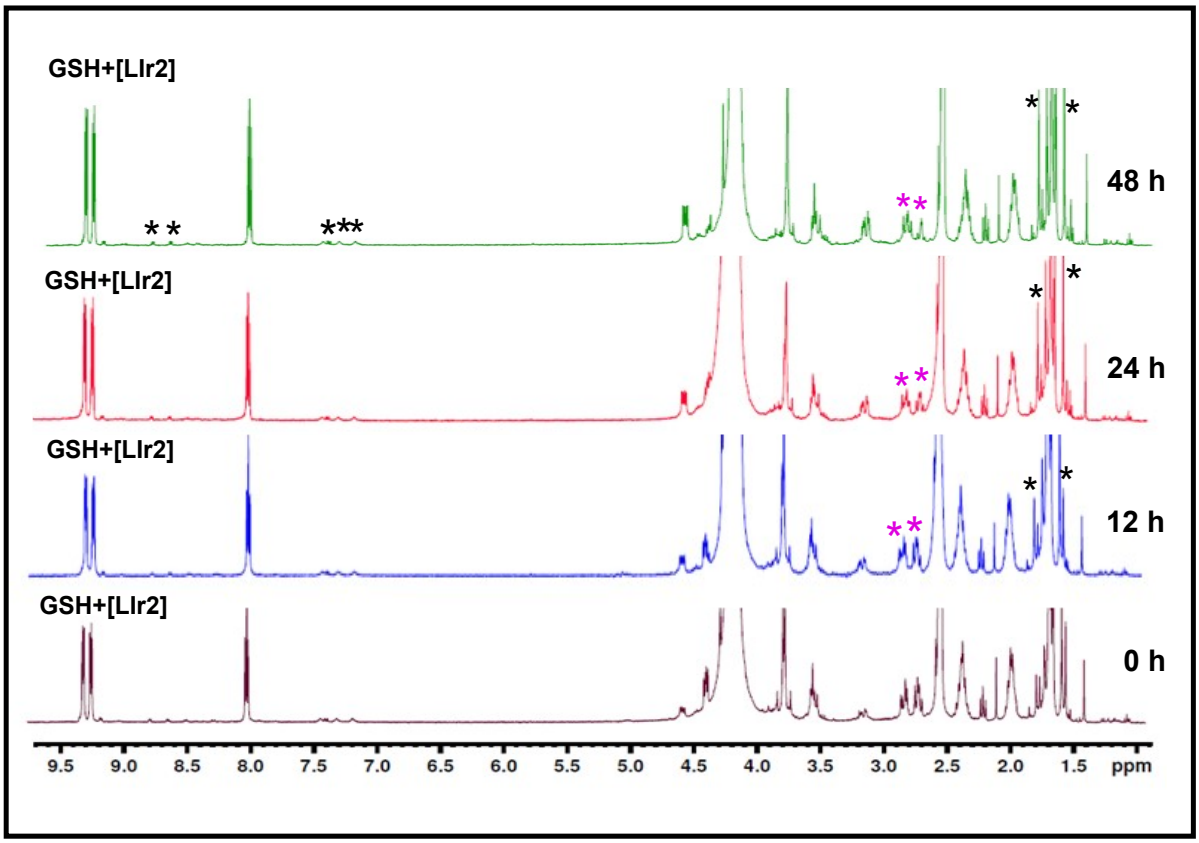
GSH+[Llr2]
48 h
GSH+[Llr2]
24 h
GSH+[Llr2]
12 h
GSH+[Llr2]
0 h
9.5 9.0 8.5 8.0 7.5 7.0 6.5 6.0 5.5 5.0 4.5 4.0 3.5 3.0 2.5 2.0 1.5 ppm

(c)

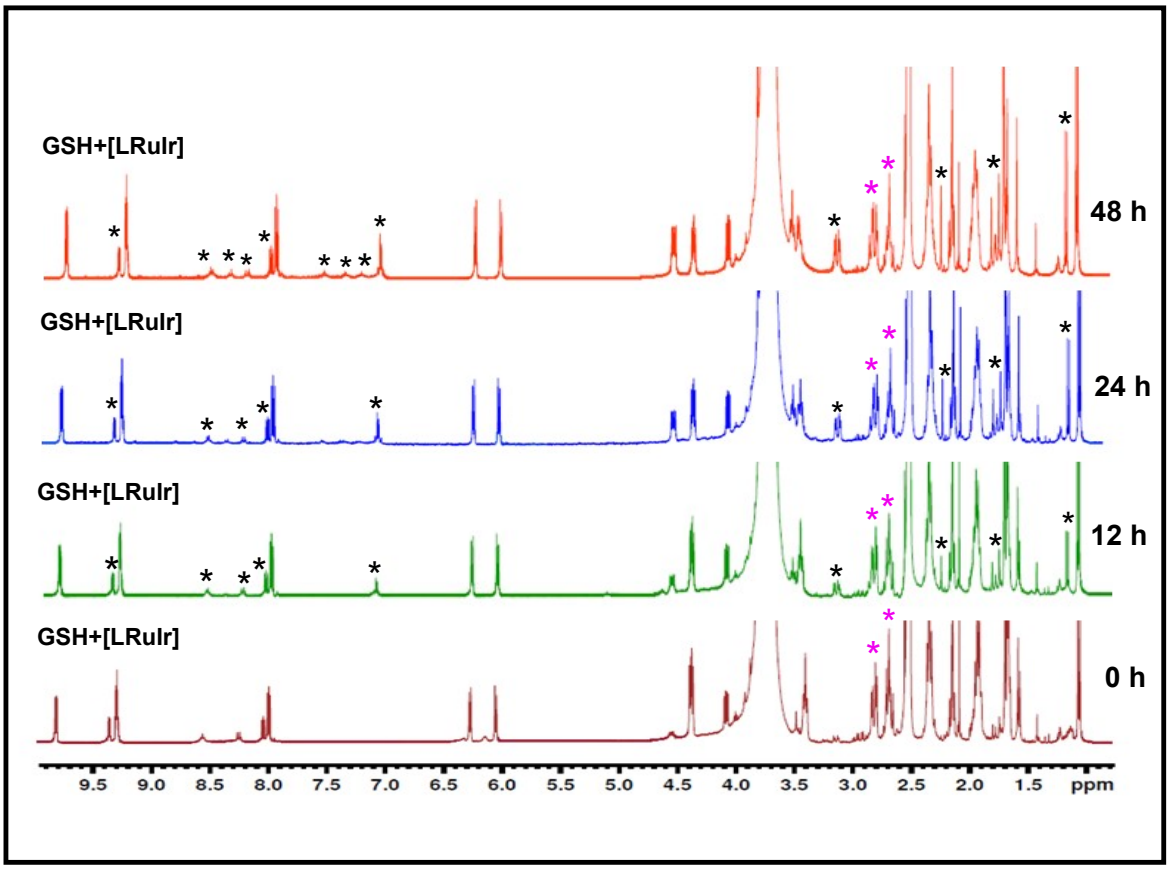

Fig. S4 Stability study of complex (a) LRu2 (b) LIr2 and (c) LRuIr in reduced L-glutathione and water *via* ^{1}H NMR. Complexes are mixed with reduced L-glutathione (middle three) in 30% DMSO-d_6/D_2O mixture, recorded at different interval of time (0h, 12h, 24h and 48h) at 25°C. t = 0 h, stands for the spectra recorded immediately after dissolving reduced L-glutathione and complex. *stands for hydrolysis product, *stands for GSH auto-oxidation product.

(a)

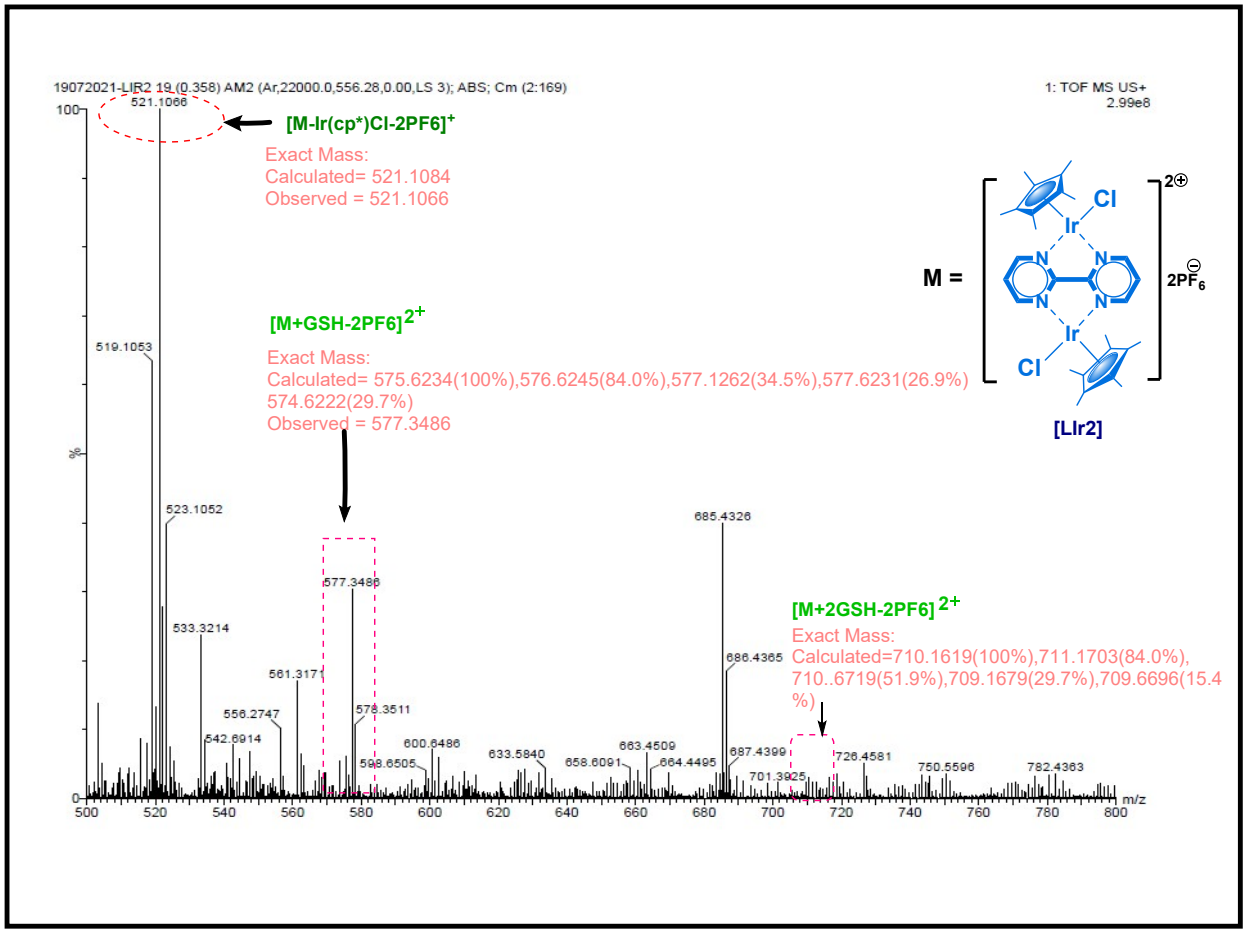
19072021-LIR2 19.(0.358) AM2 (Ar,22000.0,556.28,0.00,LS 3); ABS; Cm (2:169)
1: TOF MS US+
2.99e8
521.1066
[M-Ir(cp*)Cl-2PF6]+
Exact Mass:
Calculated= 521.1084
Observed = 521.1066
M =
Cl
Ir
N
N
N
N
Ir
Cl
2⊕
2PF6⊖
[LIr2]
[M+GSH-2PF6]2+
Exact Mass:
Calculated= 575.6234(100%),576.6245(84.0%),577.1262(34.5%),577.6231(26.9%)
574.6222(29.7%)
Observed = 577.3486
519.1053
523.1052
533.3214
561.3171
556.2747
542.6914
577.3486
578.3511
598.6505
600.6486
633.5840
658.6091
663.4509
664.4495
685.4326
686.4365
687.4399
701.3925
726.4581
750.5596
782.4363
[M+2GSH-2PF6]2+
Exact Mass:
Calculated=710.1619(100%),711.1703(84.0%),
710..6719(51.9%),709.1679(29.7%),709.6696(15.4
%)
100
%
0
500
520
540
560
580
600
620
640
660
680
700
720
740
760
780
800
m/z

(b)

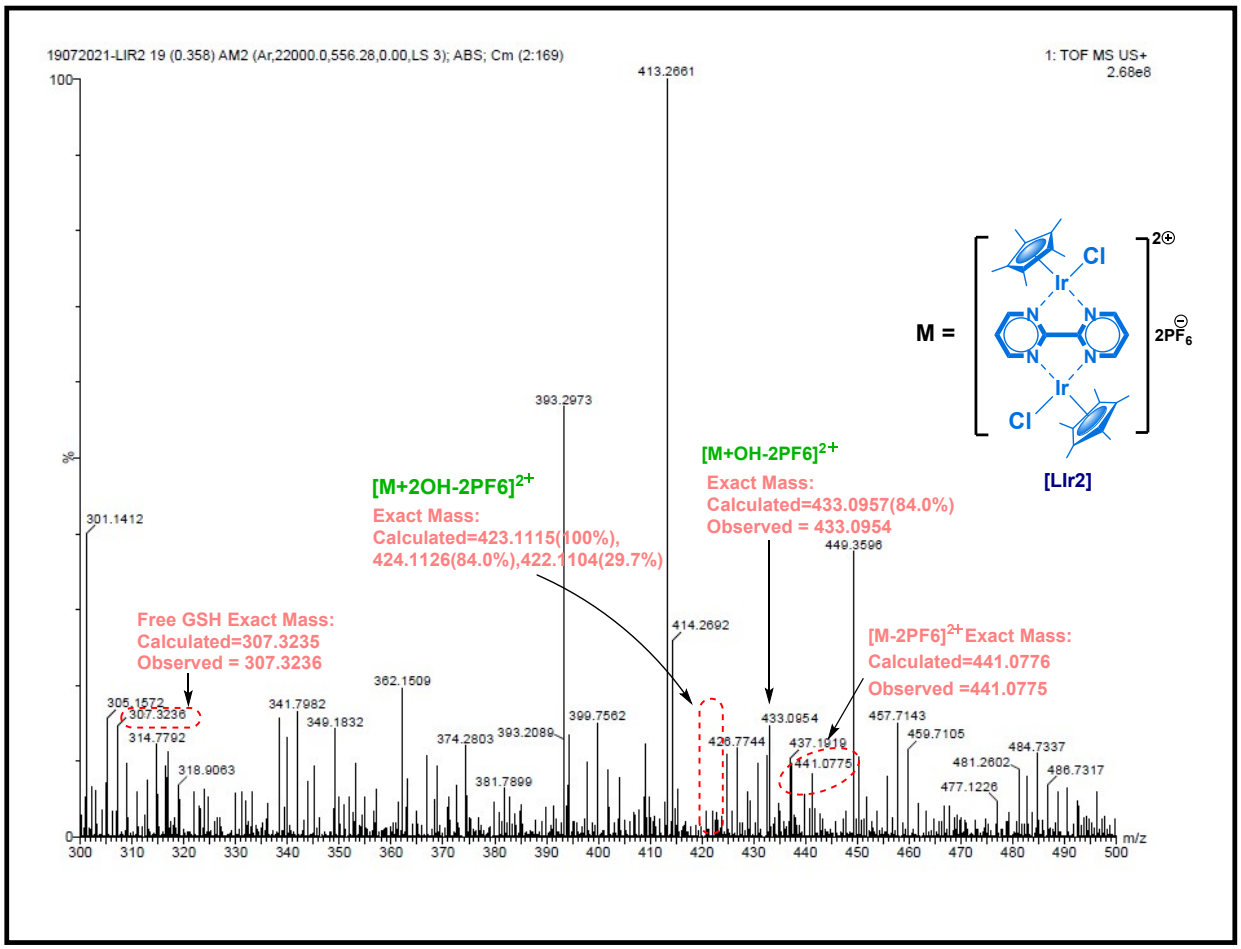
19072021-LIR2 19 (0.358) AM2 (Ar,22000.0,556.28,0.00,LS 3); ABS; Cm (2:169)
1: TOF MS US+
2.68e8
M =
Cl
Ir
N
2PF6
[LIr2]
[M+2OH-2PF6]2+
Exact Mass:
Calculated=423.1115(100%),
424.1126(84.0%),422.1104(29.7%)
[M+OH-2PF6]2+
Exact Mass:
Calculated=433.0957(84.0%)
Observed = 433.0954
Free GSH Exact Mass:
Calculated=307.3235
Observed = 307.3236
[M-2PF6]2+ Exact Mass:
Calculated=441.0776
Observed =441.0775
m/z

(c)

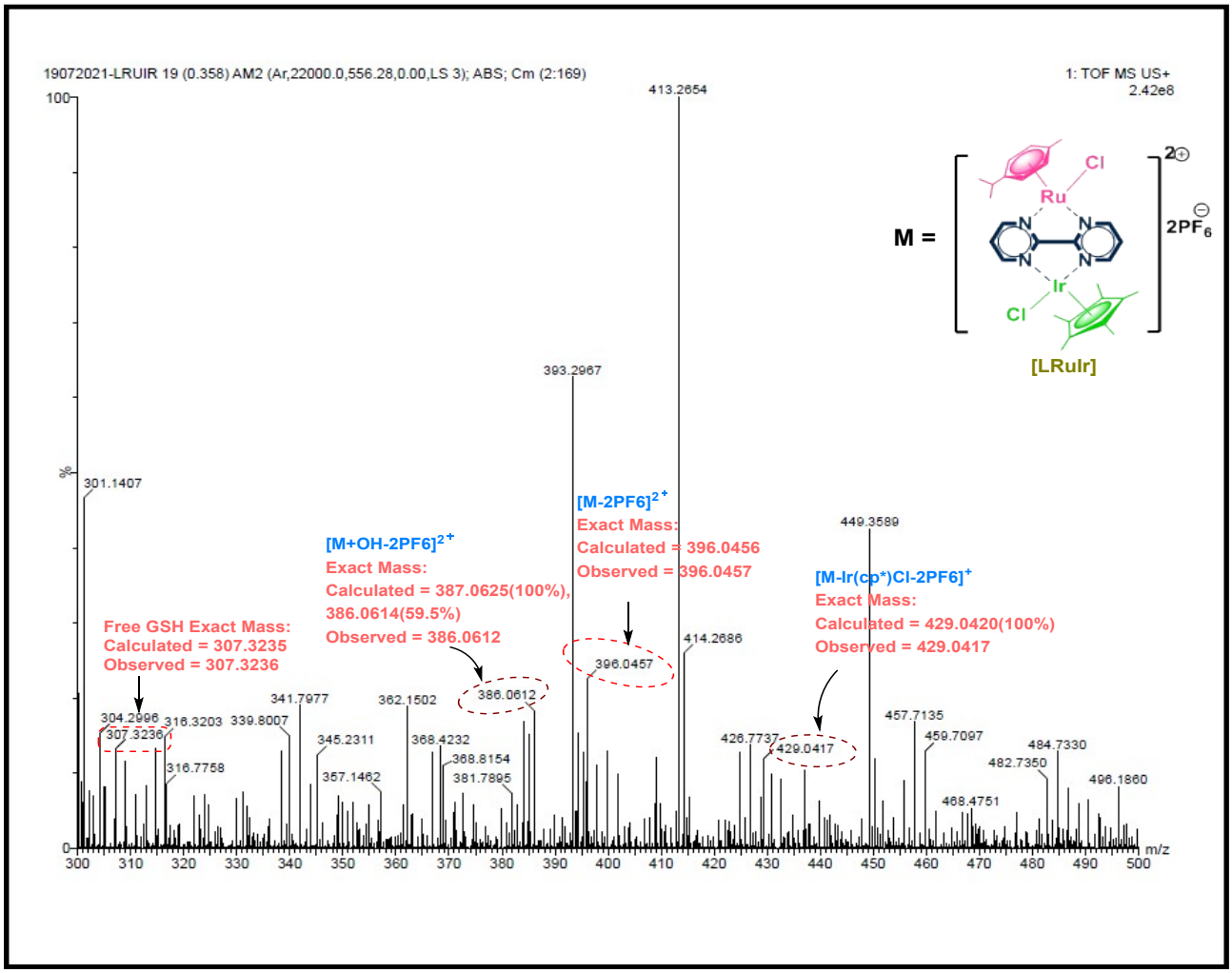
19072021-LRUIR 19 (0.358) AM2 (Ar,22000.0,556.28,0.00,LS 3); ABS; Cm (2:169)
1: TOF MS US+
2.42e8
M =
Cl
Ru
N
N
N
N
Ir
Cl
2⊕
2PF6⊖
[LRuIr]
[M+OH-2PF6]2+
Exact Mass:
Calculated = 387.0625(100%),
386.0614(59.5%)
Observed = 386.0612
[M-2PF6]2+
Exact Mass:
Calculated = 396.0456
Observed = 396.0457
[M-Ir(cp*)Cl-2PF6]+
Exact Mass:
Calculated = 429.0420(100%)
Observed = 429.0417
Free GSH Exact Mass:
Calculated = 307.3235
Observed = 307.3236
413.2654
393.2967
301.1407
449.3589
414.2686
396.0457
386.0612
362.1502
341.7977
339.8007
316.3203
304.2996
307.3236
316.7758
345.2311
357.1462
368.4232
368.8154
381.7895
426.7737
429.0417
457.7135
459.7097
484.7330
482.7350
496.1860
468.4751
%
m/z

(d)

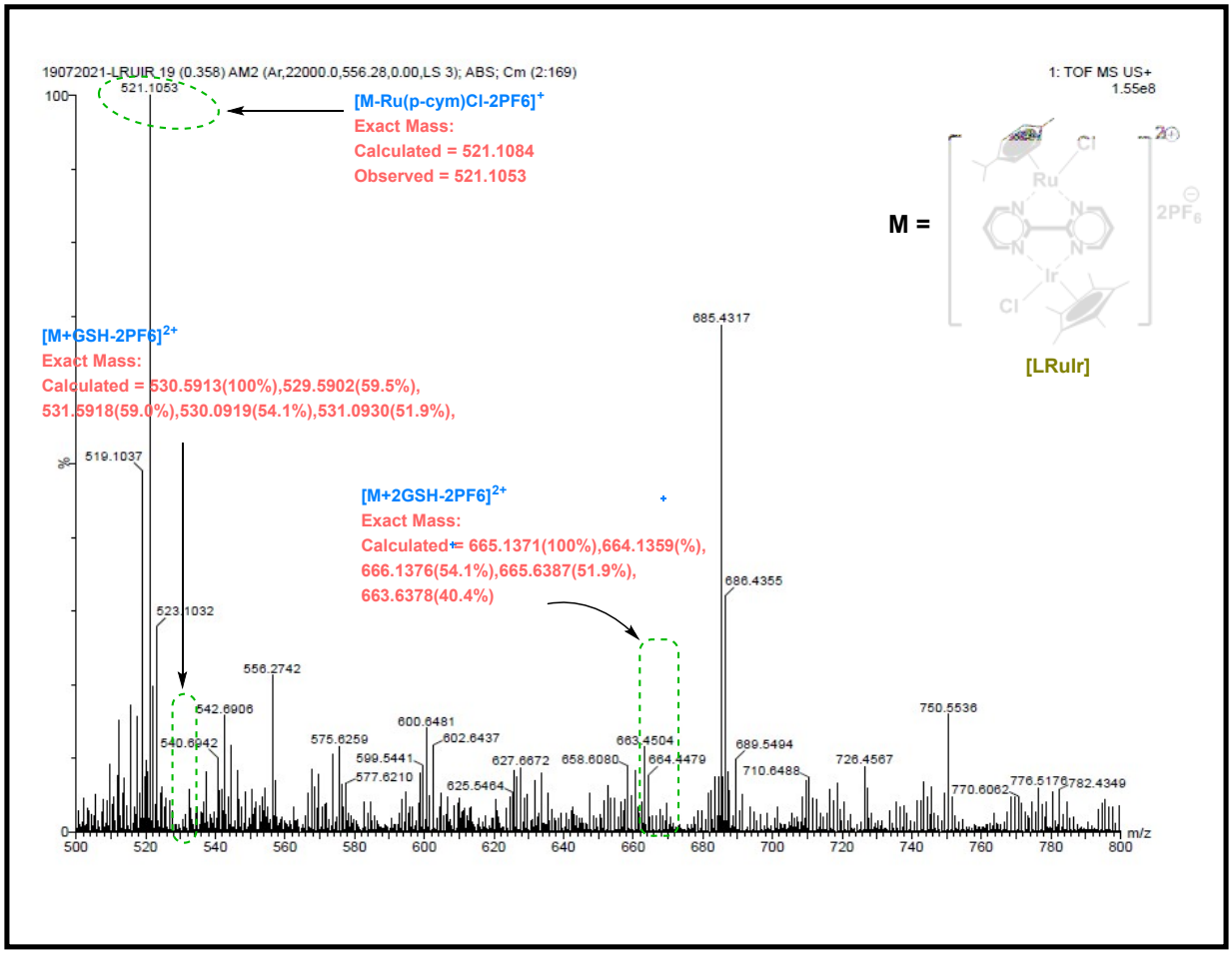

Fig. S5 HRMS of GSH binding adduct with a) and b) complex [LIr2]; c) and d) complex [LRuIr], after incubation for 30 min of complex with 10 equivalent of GSH.

Ct-DNA Binding Study

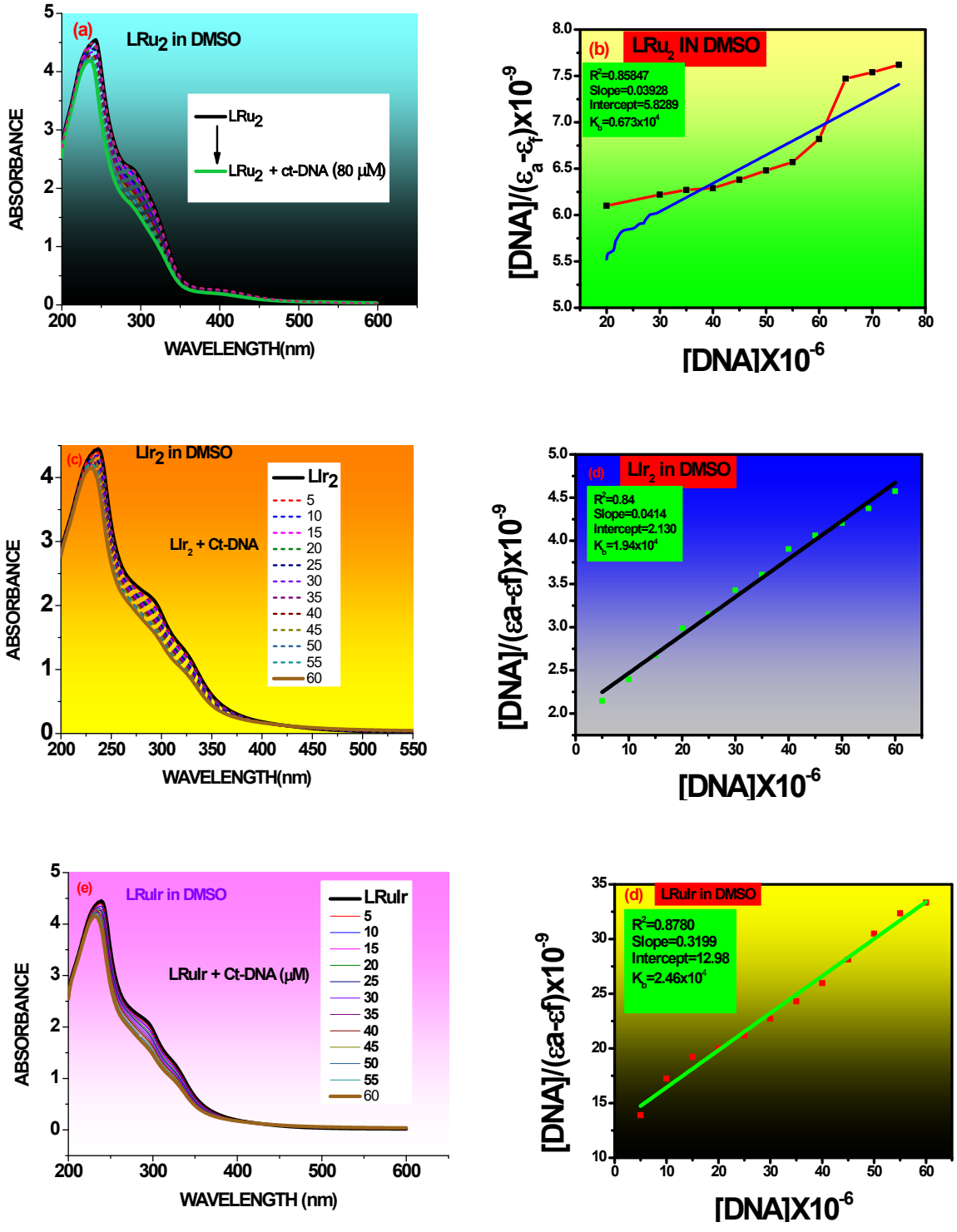

Fig. S6 Absorption spectral traces for complex (a) [LRu_2], (c) [LIr_2] and (e) [LRuIr] with increasing concentration of CT-DNA in DMSO medium (b, d, f) Plot associated with the titration of [LRu_2], [LIr_2], [LRuIr] and CT-DNA at 298 K for liner fitting to calculate K_b

EtBr Quenching study

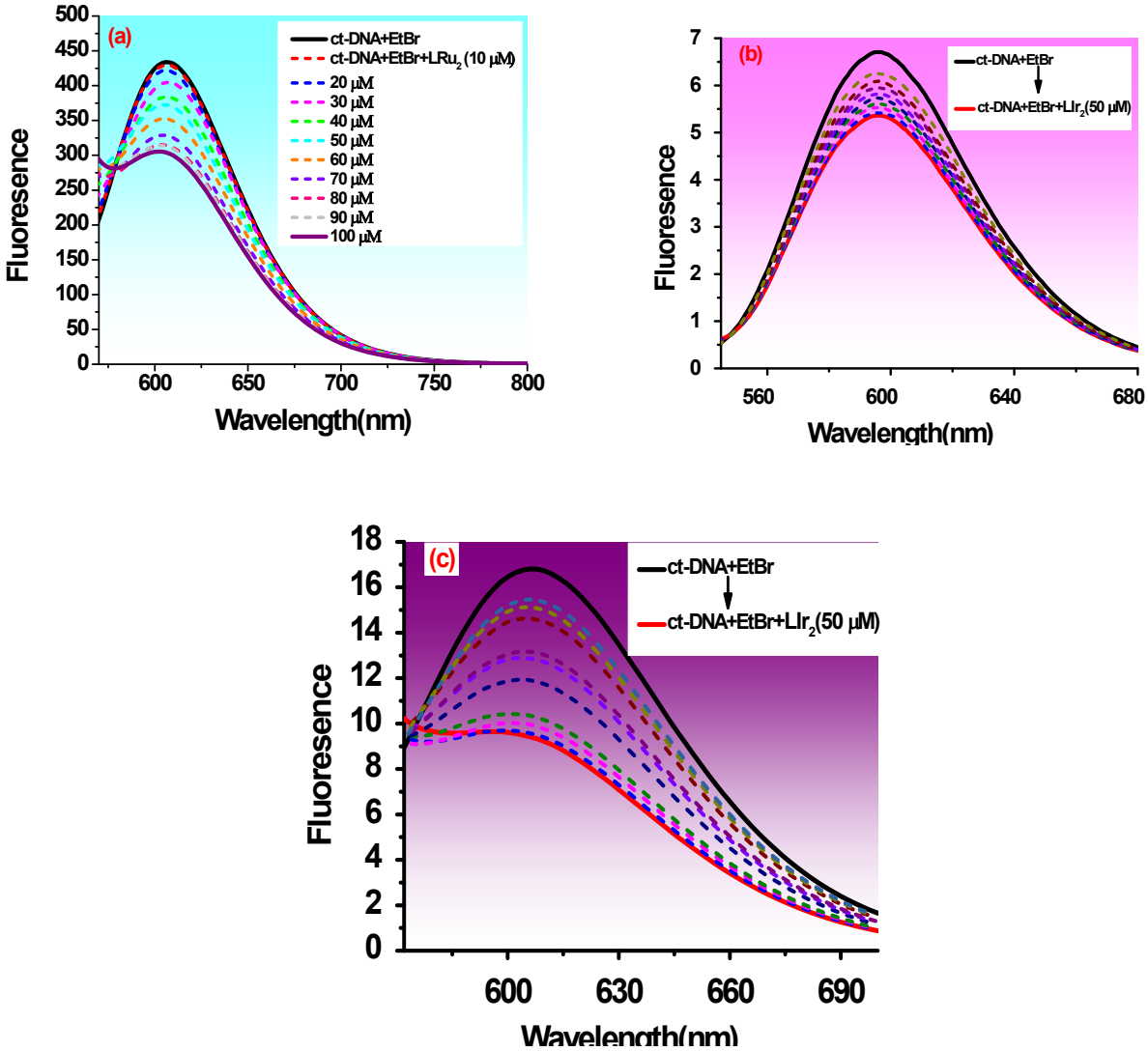

Fig.S7 Fluorescence quenching of EtBr-DNA with complex (a) [LRu_2] (c) [LIr_2] and (e) [LRuIr] with an increase in concentration of the complexes.

Table S3. DNA binding parameters for bimetallic complexes([**LRu_2**], [**LIr_2**]and[**LRuIr**])with CT-DNA

Complex	Δε (%)[a]	K_b($\times10^5$ M^{-1})[b]	K_{app}($\times10^6$ M^{-1})[c]
LRu_2	24	0.067	1.3
LIr_2	30	0.194	1.6
LRuIr	32	0.246	2.0

[a]% of Change in hypochromism; [b]K_b, intrinsic DNA binding constant from UV–visible absorption titration; [c]K_{app}, apparent DNA binding constant from competitive displacement

BSA binding Study

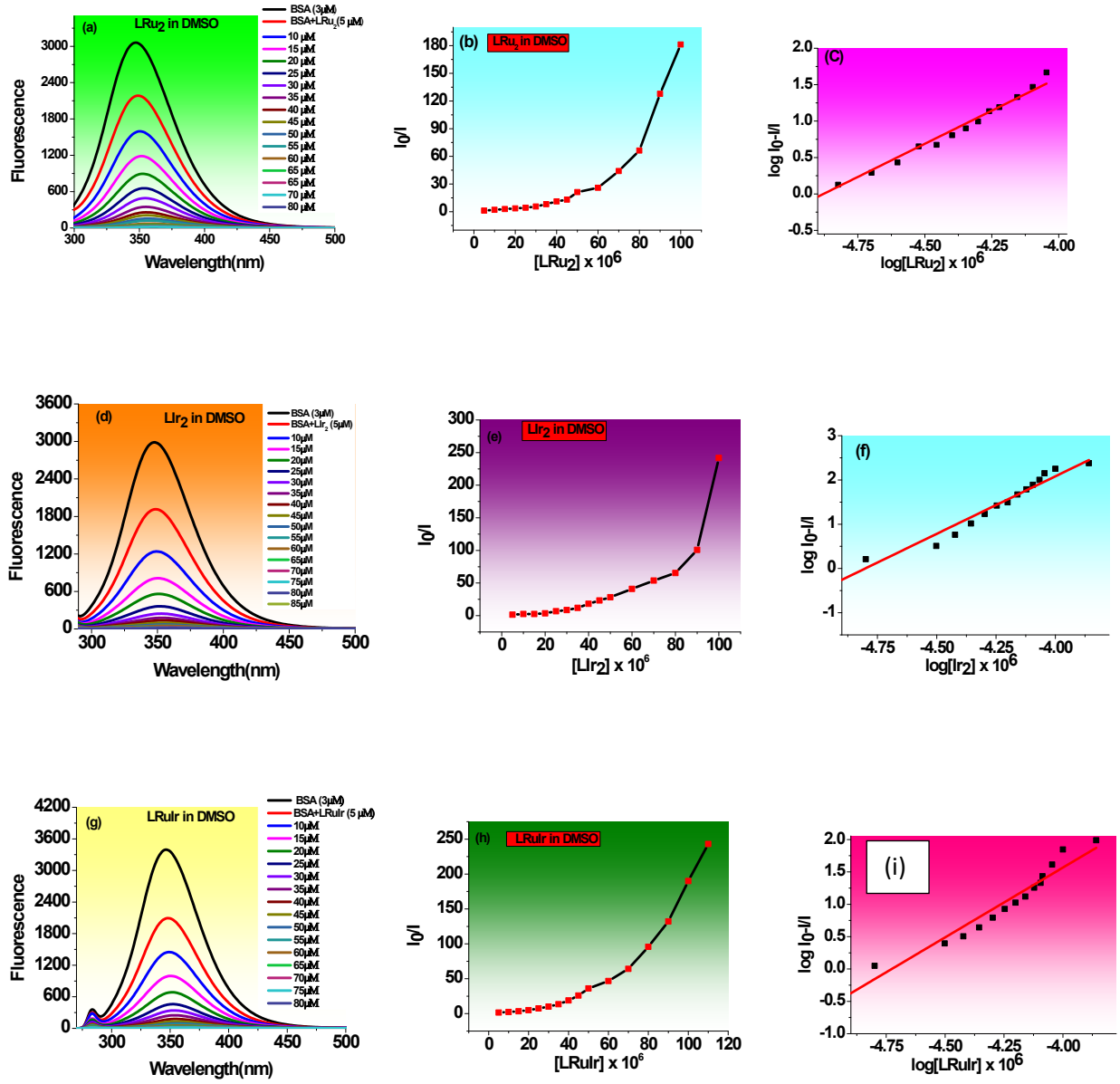

Fig. S8 Fluorescence quenching of BSA on addition of increasing concentration of the complexes (a) [LRu_2] (d) [LIr_2] and (g) [LRuIr] in DMSO.Plot of I_0/I vs. concentrations of complexes (b) [LRu_2], (e) [LIr_2] and (h) [LRuIr] in DMSO medium.Scatchard plot of log([I_0-I]/I) vs. log[complex] for BSA in the presence of complexes (c) [LRu_2], (f) [LIr_2] and (i) [LRuIr] in DMSO medium

Table S4: Binding parameters for the interaction of complexes **[LRu$_2$]**, **[LIr$_2$]**and**[LRuIr]**with BSA

Complex	K_{BSA} (M^{-1})[a]	K_q[b]	K(M^{-1})[c]	n_{BSA}[d]
[LRu$_2$]	1.5±0.24 x 10^6	1.5±0.24 x 10^{14}	8.9 x 10^5	1.81± 0.34
[LIr$_2$]	1.75±0.33x 10^6	1.75±0.33 x 10^{14}	5.6 x 10^5	2.59± 0.1
[LRuIr]	2.06±0.22 x 10^6	2.06±0.22 x 10^{14}	3.9 x 10^5	2.15± 0.13

[a]K_{BSA}, Stern Volmer quenching constant; [b]K_q, quenching rate constant (BSA); [c]K, binding constant with BSA, n_{BSA}[d], number of binding sites (BSA)

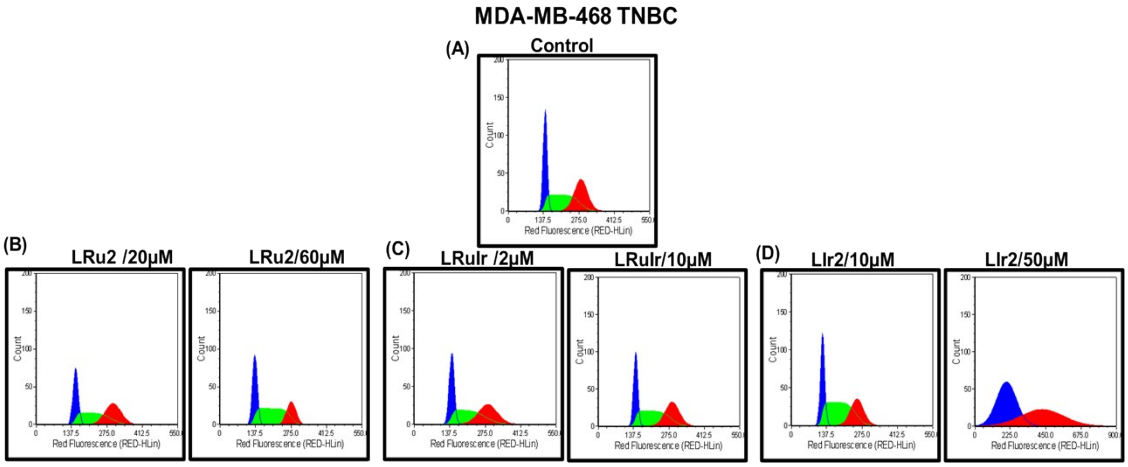

Fig. S9 Effect of the complexes in cell cycle of TNBC line. A) Cell cycle of a control breast cancer cell line. B) effect of [LRu$_2$] C) [LRuIr] and D) [LIr$_2$]complexes on cell cycle of TNBC

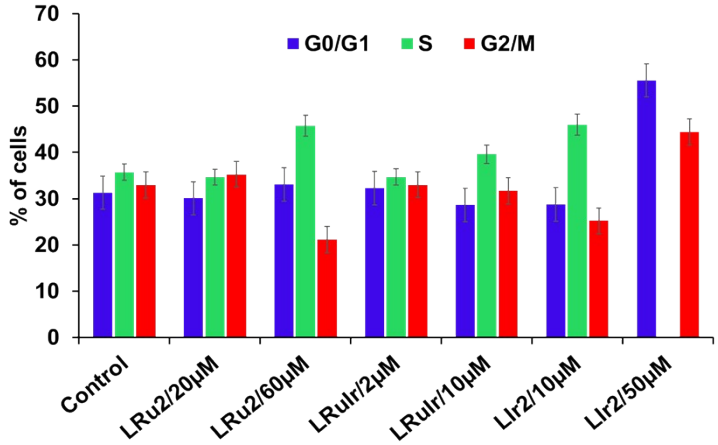

Fig. S10 Graphical representation of the cell cycle status of TNBC line up on treatment with three complexes [LRu$_2$], [LRuIr] and [LIr$_2$]. Error bars indicate mean ± SD, and represent at least three independent experiments.

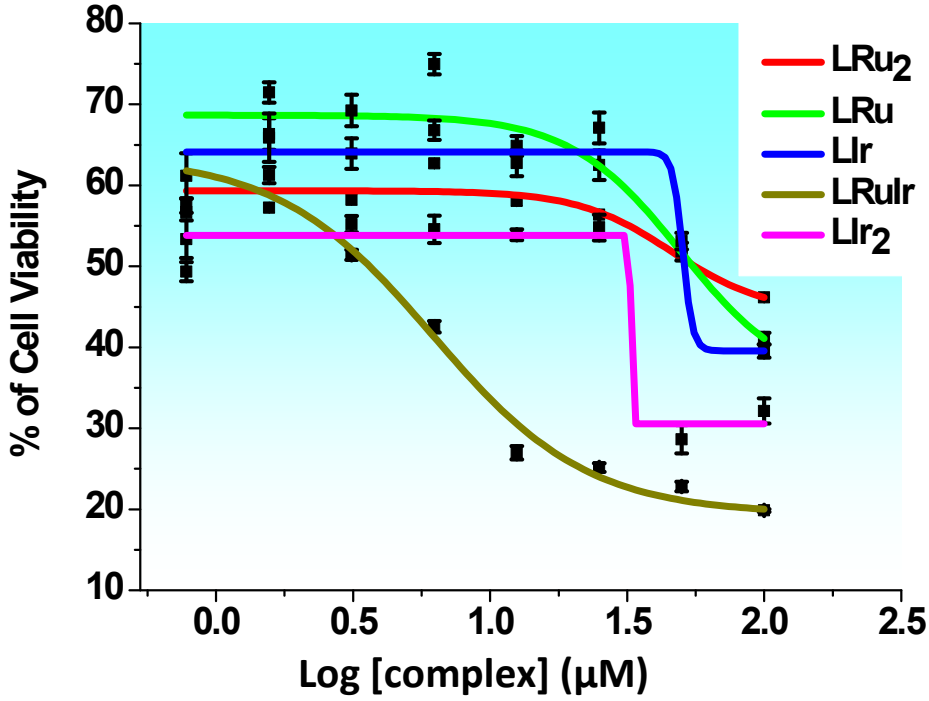

Fig. S11: MTT assay and IC_{50} value determination of Caco-2 cells up on treatment with [LRu], [LIr],[LRu_2], [LIr_2] and [LRuIr]

Experimental Procedure

Materials and methods

In our study highest commercial quality reagents and solvents were used. Bipyrimidine, $[(\eta^6\text{-}p\text{-cymene})RuCl(\mu\text{-}Cl)]_2$ and $[(\eta^5\text{-}Cp^*)IrCl(\mu\text{-}Cl)]_2$ were procured from SPECTROCHEM and Sigma Aldrich Chemical Ltd, MERK. ct-DNA, bovine serum albumin (BSA) wasobtained from Sigma Aldrich Chemical Limited. Caco-2, MDA-MB-468, MCF-10A cell lines were purchased from NCCS, Pune. DMEM medium, 1% penicillin, streptomycin and 1% of Glutmax were purchased from Gibco. 10% fetal bovine serum and 0.25% trypsin-EDTA were procured from Himidia and Thermo Fisher Scientific, USA respectively.NMR spectra were recorded on a 400 MHz Advance Bruker DPX spectrometer with tetramethylsilane (TMS) as internal standard. The chemical shifts were reported in ppm units. Abbreviations are as follows: s, singlet; d, doublet; dd, double doublet; t, triplet; m, multiplet. Elchem Microprocessor based DT apparatus was used to measurethe melting points of the complexes. TLC was accomplished on silica gel

60 F_{254} pre-coated aluminum sheets (E. Merck, Germany) using the solvent system hexane, ethylacetate, methanol solvents and spots were envisaged using UV lamp. Infrared spectra (IR) were carried out on a Shimadzu Affinity FT-IR spectrometer in the range of 4000–400 cm^{-1}. The mass spectra of the synthesized compounds were recorded on Applied Biosystems (API-4000 ESI-mode), using methanol as solvent. UV-Visible spectra and fluorescence spectra were recorded on a JASCO V-760 spectrometerand Hitachi F7000 fluorescence spectrophotometer respectively. TDS Conductometer was used to measure the Conductivity.Elisa reader and 96-well plate was used for MTT assay.

Synthesis of [(η^6-*p*-cymene)$Ru^{II}Cl(K^2$-N,N-L)]PF_6 ([LRu])

25 mg (0.041 mmole, 0.5 equivalent) of [(η^6-*p*-cymene)RuCl(μ-Cl)]$_2$ was dissolved in 5 ml of methanol in a round bottom flask. Then 13 mg (1.1 equivalent) of bipyrimidine was added to the reaction mixture and sonicated for 2 h at ambient temperature. Once the colour of the solution changed from deep yellow to deep red, 14 mg (1.1 equivalent) of NH_4PF_6 was added to the reaction mixture and stirred for another 2 h. The reaction was monitored by TLC by 100% methanol as solvent system. After the complete conversion, methanol was evaporated and obtained solid crude product was washed thoroughly with 5 ml of hexane followed by drying. The purified product was crystalized from methanol-diethyl ether mixture and red coloured fine crystals were obtained with 94% yield. The structure of [**LRu**]was examined by ^1H, ^{19}F, and ^{31}P NMR, FT-IR and ESI-MS. Purity of the sample was determined by CHN analysis.

[(η^6-*p*-cymene)$Ru^{II}Cl(K^2$-*N,N*-bipyrimidine)]PF_6 ([LRu]): 44 mg (0.076 mmol, 94%); *Mr* ($C_{18}H_{20}N_4ClF_6PRu$) = 573.87 g/mol; Anal. Calcd for $C_{18}H_{20}N_4ClF_6PRu$: C 37.67, H 3.51, N 9.76; Found: C 37.88; H 3.72; N 9.44;Yield: 94%; Mp: 200-202^oC; R_f (100% Methanol): 0.44; ^1H NMR (DMSO-d_6, 400 MHz): δ 9.89(d, *J* = 4.8 Hz, 2H, H-6, H-1), 9.32 (t,*J* = 3.2 Hz, 2H, H-3, H-8), 8.03 (t, *J* = 5.6 Hz, 2H, H-2, H-7), 6.34 (d, *J* = 6.0 Hz, 2H, H-c, H-d), 6.11 (d, *J* = 6.4 Hz, 2H, H-e, H-f), 2.66-2.78 (sep, 1H, H-h), 2.14 (s, 3H, H-a), 1.07 (d, *J* = 6.8 Hz, 3H, H-i, H-j); ^{19}F NMR (DMSO-d_6, 376 MHz): δ -66.28 (PF_6), -64.39 (PF_6); ^{31}P NMR (DMSO-d_6, 162 MHz): δ -152 to -126 (PF_6); IR (cm^{-1}, KBr): 3132 (Arm C-H stretching), 1573 (Arm

C=C stretching), 1357 (C-N stretching), 1199.7 (C-H stretching), 827 (P-F stretching), 734(C-H bending); ESI-MS (MeOH): m/z: 429.4 $[M\text{-}PF_6]^+$.

Synthesis of $[(\eta^5\text{-Cp*})Ir^{III}Cl(K^2\text{-}N,N\text{-}bipyrimidine)]PF_6$ ([LIr])

25 mg (0.031mmole, 0.5 equivalent) of $[(\eta^5\text{-Cp*})IrCl(\mu\text{-Cl})]_2$was dissolved in 5 ml of methanol and and 10 mg (1.1 equivalent) of bipyrimidine was added and then it was kept for sonication for 2h in a sonicator at ambient temperature. When a change in colour from orange to light yellow was observed,12 mg i.e. 1.1 equivalent of Ammonium hexaflurophosphate was added to the mixture and again kept for sonication in a sonicator for 2 h. Progress of chemical reaction was monitored by thin layer chromatography in 100%methanol as the solvent system. After completion of the reaction the complex formed was dried under room temperature after the product formed was completely dried, the product was washed with hexane for 2 to 3 times to remove impurities present. The purified product was further crystalized from methanol/diethyl ether mixture. The yellow fine crystals were obtained with 95 % yield. The structure of [**LIr**] was confirmed by NMR, FT-IR and ESI-MS. Purity of this complex was determined by C, H, N analysis.

$[(\eta^5\text{-Cp*})Ir^{III}Cl(K^2\text{-}N,N\text{-}bipyrimidine)]PF_6$ *(*[LIr]): 40mg (0.060 mmol, 95%); *Mr* ($C_{18}H_{21}N_4IrClPF_6$) = 666.02 g/mol; Anal. Calcd for $C_{18}H_{21}N_4IrClPF_6$: C 32.46, H 3.18, N 8.41 ; Found: C 32.77; H 3.34; N 8.12;Yield: 95%; Mp: 220-222^{o}C; R_f (100% Methanol): 0.36; ^{1}H NMR (DMSO-d_6, 400 MHz): δ 9.37 (dd, *J1* = 4.8 Hz, *J2* = 2.0 Hz,2H, H-1, H-6), 9.32 (dd, *J1* = 6.0 Hz, *J2* = 2.0 Hz,2H, H-3, H-8), 8.05 (t, *J* = 5.2 Hz,2H, H-2, H-7), 1.70 (s, 15H, cp*, H-a-e); ^{19}F NMR (DMSO-d_6, 376 MHz): δ -71.05 (PF_6), -69.17 (PF_6); ^{31}P NMR (DMSO-d_6, 162 MHz): δ -152 to -135 (PF_6); IR (cm^{-1}, KBr): 3103 (Arm C-H stretching), 1577 (Arm C=C stretching), 1406 (C-N stretching), 1379 (C-H stretching), 837 (P-F stretching), 748(C-H bending), 555; ESI-MS (MeOH): m/z: 521.7 $[M\text{-}PF_6]^+$.

Synthesis of $[(\eta^6\text{-}p\text{-cymene})(\eta^5\text{-Cp*})Ru^{II}Ir^{III}Cl_2(K^2\text{-N,N-}bipyrimidine)](PF_6)_2$ ([LRuIr])

25 mg (0.031mmole, 0.5 equivalent) of $[(\eta^5\text{-Cp*})IrCl(\mu\text{-Cl})]_2$was dissolved in 5 ml of methanol and stirred for 10 min to dissolve the compound completely in methanol.

Then 1.1equivalent of previously prepared complex [**LRu**] was added to the reaction mixture and sonicated for 2 h at ambient temperature. As soon as a change in colour from orange to deep red was observed, 12 mg i.e. 1.1 equivalent of NH_4PF_6 was added to the reaction mixture and stirred for another 2 h to complete the reaction. The reaction was monitored by TLC using 100% methanol as solvent system. After the completion of the reaction, methanol was evaporated andthe impurities were removed by washing the crude product thoroughly with 5 ml of hexane followed by diethyl ether.The purified product was further crystalized from methanol/diethyl ether and the brown coloured fine crystals of compound [**LRuIr**] was obtained with 95%yield. The structure of [**LRuIr**] were analysed by NMR, FT-IR and ESI-MS. Purity of the complex was determined by C, H, N analysis.

[(η^6-*p*-cymene)(η^5-Cp*)$Ru^{II}Ir^{III}Cl_2$(K^2-N,N-*bipyrimidine*)]$(PF_6)_2$ ([LRuIr]): 46 mg (0.04 mmol, 97%); *Mr* ($C_{28}H_{35}N_4Cl_2F_{12}P_2IrRu$) = 1081.73 g/mol; Anal. Calcd for $C_{28}H_{35}N_4Cl_2F_{12}P_2IrRu$: C 31.09, H 3.26, N 5.18; Found: C 31.41; H 3.41; N 5.50;Yield: 97%; Mp: 195-198^oC; R_f (100% Methanol): 0.38; ^1H NMR (DMSO-d_6, 400 MHz): δ 9.87 (d, *J* = 4.4 Hz, 1H, H-6), 9.37 (d, *J* = 4.4 Hz, 1H, H-1), 9.32 (d, *J* = 5.2 Hz, 2H, H-3, H-8), 8.05 (dd, *J1* = 5.6 Hz, *J1* = 11.6 Hz, 2H, H-2, H-7), 6.30 (d, *J* = 6.4 Hz, 1H, H-c), 6.09 (d, *J* = 6.4Hz, 1H, H-d), 5.80 (dd, *J1* = 6.0 Hz, *J2* = 16.8Hz, 2H, H-c, H-f), 2.78-2.85 (m, 1H,*p*-cymene, H-h), 2.14 (s, 3H, *p*-cymene, H-a), 1.62 (s, 15H,Cp^*,H-a′-e′), 1.07 (d, *J* = 6.8 Hz, 3H *p*-cymene, H-i), 1.17 (d, *J* = 7.2 Hz, 3H, *p*-cymene, H-j); ^{19}F NMR (DMSO-d_6, 376 MHz): δ -71.06 (PF_6), -69.17 (PF_6); ^{31}P NMR (DMSO-d_6, 162 MHz): δ -157to -131 (PF_6); IR (cm^{-1}, KBr): 3329 (Arm C-H stretching), 1581 (Arm C=C stretching), 1415 (C-N stretching), 1029 (C-H stretching), 831 (P-F stretching), 741 (C-H bending), 555; ESI-MS (MeOH): m/z: 395.5 $[M\text{-}2PF_6]^{2+}$, 521.7 $[M\text{-}Ru(p\text{-}cym)Cl\text{-}2PF_6]^+$, 429.4 $[M\text{-}Ir(cp^*)Cl\text{-}2PF_6]^+$.

Synthesis of [(η^6-*p*-cymene)$_2Ru_2^{II}Cl_2$(K^2-*N,N-bipyrimidine*)]$(PF_6)_2$([LRu_2])

[(η^6-*p*-cymene)RuCl(μ-Cl)]$_2$ (20 mg, 0.032 mmol) was dissolved in methanol and 5.42 mg i.e. 1.05 equivalent of bipyrimidine was added and then it was kept for sonication for 2 h in a sonicator. After it got completely mixed after 2h, 15.970 mg i.e. 2.5 equivalent of Ammonium hexaflurophosphate was added to the mixture and again kept for sonication for 2 h. A colour change was observed from light orange to dark orange. Progress of

chemical reaction was monitored by thin layer chromatography using 100% methanol as solvent system. After the completion of the reaction, methanol was evaporated to get the solid product. To remove the impurities, crude product was washed thoroughly with hexane followed by diethyl ether for 2 to 3 times. After washing the product formed is dried and weighed in a weighing machine. The purified product was further crystalized from methanol/diethyl ether system and brown coloured fine crystals were obtained with 95% yield. The structures of [$\mathbf{LRu_2}$] were analysed by NMR, FT-IR and ESI-MS. Purity of these complexes were determined by C, H, N analysis.

[(η^6-*p*-cymene)$_2$Ru$_2^{II}$Cl$_2$(K^2-*N,N-bipyrimidine*)](PF$_6$)$_2$ ([LRu$_2$])*:* 30.7 mg (0.031 mmol, 95%); *Mr* ($C_{28}H_{34}N_4Ru_2Cl_2P_2F_{12}$) = 989.57 g/mol; Anal. Calcd for $C_{28}H_{34}N_4Ru_2Cl_2P_2F_{12}$: C 33.99, H 3.46, N 5.66; Found: C 34.23; H 3.58; N 5.94;Yield: 95 %; mp: 225-228°C; R_f (100% Methanol): 0.36; ^{1}H NMR (DMSO-d_6, 400 MHz): δ 9.86 (d, *J* = 4.0 Hz, 2H, H-1, H-6), 9.31 (d, 2H,H-12, H-14), 8.02 (t, *J* = 5.2 Hz, 2H, H-2, H-7), 6.30 (d, *J* = 6.0 Hz, 2H, *p*-cymene H-c, H-d), 6.08 (d, *J* = 6.0 Hz, 2H, *p*-cymene H-e, H-f), 5.29 (d, *J* = 6.0 Hz, 2H, *p*-cymene, H-c′, H-d′), 5.24 (d, *J* = 6.0 Hz, 2H, *p*-cymene, H-e′, H-f′), 2.69-2.76 (m, 2H, CH, H-h, H-h′), 2.14 (s, 6H, Me, H-a, H-a′), 1.07 (d, *J* = 7.2 Hz, 6H, *p*-cymene, H-i, H-j), 0.93 (d, *J* = 6.8 Hz, 6H, *p*-cymene, H-i′, H-j′);^{19}F NMR (DMSO-d_6, 376 MHz): δ -66.28 (PF_6), -64.39(PF_6); ^{31}P NMR (DMSO-d_6, 162 MHz): δ -152 to -126 (PF_6); IR (cm^{-1}, KBr):3132 (ArmC-H stretching), 1573 (Arm C=C stretching), 1357 (C-N stretching), 1076 (C-H stretching), 804 (P-F stretching), 734(C-H bending);ESI-MS (MeOH): m/z: 349.8 [M-2PF_6]$^{2+}$, 429.0 [M-Ru(*p*-cym)Cl-2PF_6]$^+$.

Synthesis of [(η^5-Cp*)$_2$Ir$_2^{III}$Cl$_2$(K^2-*N,N-bipyrimidine*)](PF$_6$)$_2$([LIr$_2$])

20 mgof [(η^5-Cp*)IrCl(μ-Cl)]$_2$ (0.024, 1 equivalent) was dissolved in methanol and 4.2 mg i.e 1.05 equivalent of bipyrimidine was added and then it was kept for sonication for 2 h in a sonicator. After it got completely mixed after 2 h, 8.60 mg i.e 2.05 equivalent of Ammonium hexaflurophosphate was added to the mixture and again kept for sonication in a sonicator for 2 h. Progress of chemical reaction was monitored by thin layer chromatography in 100 % methanol as the solvent system. After completion of the reaction the solvent was evaporated and the obtained crude product was completely dried followed bywashing with hexane for 2 to 3 times to remove impurities. After washing the product formed is dried and weighed in a

weighing machine. The purified product was further crystalized from methanol/diethyl ether system and brown coloured fine crystals were obtained with 96% yield. The structures of [**LIr_2**]were analysed by NMR, FT-IR and ESI-MS. Purity of these complexes were determined by C, H, N analysis.

[(η^5-Cp*)$_2$Ir$_2^{III}$Cl$_2$(K^2-*N,N-bipyrimidine*)](PF$_6$)$_2$([LIr_2]): 28 mg (0.035 mmol, 98%); *Mr* ($C_{28}H_{36}N_4Ir_2Cl_2P_2F_{12}$) = 1173.88 g/mol; Anal. Calcd for $C_{28}H_{36}N_4Ir_2Cl_2P_2F_{12}$: C 28.65, H 3.09, N 4.77; Found: C 28.89; H 3.46; N 4.92;Yield: 98%; Mp: 235-237^{o}C; R_f (100% Methanol): 0.32; ^{1}H NMR (DMSO-d_6, 400 MHz): δ 9.38 (d, 2H, *J* = 4.0 Hz, H-1, H-6), 9.32 (d, *J* = 4.8 Hz, 2H,H-3, H-8), 8.05 (t, *J* = 5.2 Hz,2H,H-2, H-7), 1.70 (s, 30H,Cp*, H-a′-e′); ^{19}F NMR (DMSO-d_6, 400 MHz): δ -71.00 (PF_6), -69.17 (PF_6); ^{31}P NMR (DMSO-d_6, 400 MHz): δ -152 to -131 (PF_6); IR (cm^{-1}, KBr): 3541 (Arm C-H stretching), 1579 (Arm C=C stretching), 1402 (C-N stretching), 1026, 835 (P-F stretching), 748 (C-H bending), 555; ESI-MS (MeOH): m/z: 441.4 $[M\text{-}2PF_6]^{2+}$, 521.5 $[M\text{-}Ir(cp^*)Cl\text{-}2PF_6]^+$.

Cell culture:

Human triple negative breast cancer (TNBC) cell line (MDA-MB-468), was procured from the National centre for cell science (NCCS), Pune. MDA-MB-468 cells were maintained in DMEM media (Gibco) supplemented with 10% fetal bovine serum (Himedia, India), 1% penicillin and streptomycin and 1% of Glutmax (Gibco, Thermo Scientific, USA) at 37 °C in 5% CO_2. The cells were trypsinized upon reaching 70–80% confluency using 0.25% trypsin-EDTA (Thermo Fisher Scientific, USA). Similarly, Caco-2 cells were also maintained in DMEM media (Gibco) supplemented with 20% fetal bovine serum (Himedia, India).

***In vitro* cytotoxicity study in Caco-2 and MDA-MB-468**

In vitro cytotoxicity was evaluated by standard MTT assay protocol.[1] Synthesized complexes were dissolved in 0.1% DMSO and then serially diluted with DMEM medium. Approximately 1×10^4 cells for CaCo-2 and 5000 cells for MDA-MB-468per well were cultured in 100 µl of a growth medium in 96-well plates and incubated at 37°C under 5% CO_2 atmosphere. The cells were then treated with different concentrations (1-100 µM for Caco-2 and 1-500 µM for MDA-MB-468)of the synthesized complexes (for Caco-2 all the complexes and for MDA-MB-468 only bimetallic complexes were assayed).

Cisplatin had been used as standard positive control drugs. After 48 h, the medium was superfluous and cell cultures were incubated with 100 µl MTT reagent (5 mg/mL in PBS, final concentration 0.5mg/ml) for 5 h at 37^{o} C. Then the suspension was placed on micro vibrator for 10 min followed by recording the absorbance at λ = 570 on MULTISCAN sky plate reader (Thermo scientific). The experiment was also accomplished in triplicate. The data were represented as the growth inhibition percentage i.e. % growth inhibition = 100 − [(AD × 100)/AB], where AD, measured absorbance in wells which contain samples and AB, measured absorbance for blank wells (cells with a medium and a vehicle).

Cell cycle analysis:

For cell cycle analysis, approximately 1 million MDA-MB-468 cells were treated with the drug [**LRu_2**], [**LRuIr**] and [**LIr_2**] at different concentrations (0, 20, 60µM), (0, 2, 10 µM) and (0, 10, 50 µM) respectively. After 48 h of treatment, the cells were fixed with chilled 70% ethanol for 2 h. Fixed cells were washed with PBS and stained with 500µl of the FxCycle™ PI/ RNase solution (Thermo Fisher Scientific, USA) for 30 min in dark. The cells were analysed using Guava EasyCyte Flow Cytometer (Millipore Sigma, USA). Untreated MDA-MB-468 cells were taken as control. Serum starvation for 6 h was given prior to the treatment. Cell cycle data was analysed by FCS express 5.0 software (by De Novo software) and quantification was done by using GraphPad prism software.

Annexin V FITC assay:

Apoptosis was evaluated using PI/Annexin-V-FITC apoptosis detection kit (Invitrogen, Thermo Fisher). Briefly, cells cultured in 6 well plates were trypsinized, washed, stained with Annexin V-FITC and PI for 15 mins at room temperature in dark, and then analysed by guava easyCyte flow cytometer (Merck, Germany). This assay was repeated in 3 independent experiments and the data was analysed by FCS express 5.0 software (by De Novo software).

Statistical analysis:

For comparison among two groups student t-test was performed and for multiple groups, one-way analysis of variance (ANOVA) followed by the Bonferroni post hoc test was utilized using the GraphPad Prism version 7 software. The P values of >0.12 (ns),

0.033(*), 0.002(**), <0.0002(***) were considered as significant. Error bar represents the ± standard error of mean (SEM).

Stability study[2]

UV method

The stability of the metal complexes ([**LRu$_2$**], [**Lr$_2$**] and [**LRuIr**]) was tested in 10% DMSO in water and aqueous GSH (1mM) medium upto 48 hour.

HRMS method

Stability studies were also observed in ESI Mass spectrometry. Complexes with 10 equiv. GSH in buffer which was incubated for half an hour at 37°C under stirring condition, diluted with water and ESI mass spectrometry was performed.

NMR spectroscopic method

Stability studies of these complexes with reduced L-glutathione were monitored by ^{1}H NMR. The samples were prepared in a degassed a D_2O/ DMSO-d_6 (7:3 *v/v*) mixture at ambient temperature under nitrogen atmosphere to minimize the auto oxidation of glutathione. The ratio between complex and GSH was 1:2. The binding was monitored up to 48 hours.

DNA binding study

The binding of these complexes with calf-thymus DNA (ct-DNA) were measured by electronic spectra and competitive binding assay using ethidium bromide (EtBr) as quencher by fluorescence spectroscopy.

UV–visible studies

DNA binding assay was carried out by using complexes [**LRu$_2$**], [**LIr$_2$**] and [**LRuIr**] in Tris-HCl buffer (5 mMTris-HCl in water, pH 7.4) in water medium.[3] The concentration of ct-DNA was calculated from its absorbance intensity at 260 nm and its known molar absorption coefficient value 6600 M^{-1} cm^{-1}. Equal amount of DNA was taken both in the

sample and reference in cuvettes. Titration was carried out by increasing concentration of ct-DNA. The intrinsic DNA binding constant (K_b) was calculated using the equation (i):

$$\frac{[DNA]}{(\varepsilon_a - \varepsilon_f)} = \frac{[DNA]}{(\varepsilon_b - \varepsilon_f)} + \frac{1}{K_b(\varepsilon_a - \varepsilon_f)} (i)$$

Where [DNA] is the concentration of DNA in the base pairs, ε_a is the apparent extinction coefficient observed for the complex, ε_f corresponds to the extinction coefficient of the complex in its free form, and ε_b refers to the extinction coefficient of the complex when fully bound to DNA. Data were plotted using Origin 8.5 software to obtain the [DNA]/(ε_a-ε_f) vs. [DNA] linear plot. The ratio of the slope to intercept from the linear fit gives the value of the intrinsic binding constant (K_b).

UV and Fluorescence study

Photophysical behaviour of the complexes was investigated by accomplishing UV and Fluorescence study of all these complexes in (1:9, v/v) dimethylsulfoxide (DMSO): water mixture. Fluorescence quantum yields (Φ) were calculated by using the comparative William's method which involves the use of well-characterized standard with the known quantum yield value using 10% DMSO in PBS buffer solution.[4] Quinine sulphate is used as a standard. Quantum yield was calculated according to the equation (ii):

$$\varphi = \varphi_R \times \frac{I_S}{I_R} \times \frac{OD_R}{OD_S} \times \frac{\eta_S}{\eta_R} \cdots\cdots\cdots (ii)$$

Where, φ = quantum yield, I = peak area, OD = absorbance at $\lambda_{max,}$ η = refractive index of solvent (s) and reference (R). Here, we have used quinine sulphate as a standard for calculating the quantum yield.

Ethidium bromide displacement assay

The ethidium bromide (EtBr) displacement assay was accomplished to explain the mode of binding between the potent compounds with DNA.[5] The apparent binding constant (K_{app}) of the complexes [**LRu$_2$**], [**LIr$_2$**] and [**LRuIr**] to ct-DNA were calculated using ethidium bromide (EtBr) as a spectral probe in 5 mMTris-HCl buffer (pH 7.4).

EtBr does not exhibit any fluorescence in its free form as its fluorescence is quenched by the solvent molecules. But its fluorescence intensity increases in presence of ct-DNA, which suggests the intercalative mode of binding of EtBr with DNA grooves. The fluorescence intensity was found to decrease with further increase in concentration of the complexes. Thus it can be said that the complexes displace EtBr from ct-DNA grooves and in turn complexes get bound to the DNA base pairs. The values of the apparent binding constant (K_{app}) were obtained by using the equation (iii):

$$K_{app} \times [Complex]_{50} = k_{EtBr} \times [EtBr] \cdots\cdots\cdots (iii)$$

Where K_{EtBr} is the EtBr binding constant (K_{EtBr} = 1.0 x 10^7 M^{-1}), and [EtBr] = 8 x 10^{-6} M. Stern-Volmer equation has been employed for quantitative determination of the Stern-Volmer quenching constant (K_{SV}).[6] Origin (8.5) software was used to plot the fluorescence data to obtain linear plot of I_0/I vs. [complex]. The value of K_{SV} was calculated from the following equation.

$$I_0/I = 1 + K_{SV}[Q] \quad (iv)$$

Where I_0 = fluorescence intensity in absence of complex and I = fluorescence intensities in presence of complex concentration [Q].

BSA binding studies

Serum albumin proteins are the key components in blood plasma proteins and play significant roles in drug transport and metabolism.[7] The interaction of the complex with bovine serum albumin (BSA), a structural homologue of human serum albumin (HSA), has been studied from tryptophan emission quenching experiment. Tryptophan emission quenching experiment was performed to detect the interaction of the complexes [**LRu_2**], [**LIr_2**] and [**LRuIr**] with protein BSA. Initially, BSA solution (2 x 10^{-6} M) was prepared in Tris-HCl/NaCl buffer. The aqueous solutions of the complexes were subsequently added to BSA solution with increase their concentrations. After each addition, the solutions were shaken slowly for 5 min before recording the fluorescence at a wavelength of 295 nm (λ_{ex} = 295 nm). A gradual decrease in fluorescence intensity of BSA at λ = 340 nm was observed upon increasing the concentration of complex, which confirms that the interaction between the complex and BSA is being occurred. Stern-Volmer equation has been employed to quantitatively determine the quenching

constant (K_{BSA}). Origin Lab, version 8.5 was used to plot the emission spectral data to obtain linear plot of I_0/I vs. [complex] using following equation (v):

$$I_0/I = 1 + \mathrm{K}_{BSA}[Q] = 1 + k_q\tau_0[Q] \quad (v)$$

Where I_0 is the fluorescence intensity of BSA in absence of complex and I indicates the fluorescence intensities of BSA in presence of complex of concentration [Q], τ_0 = lifetime of the tryptophan in BSA found as 1 x 10^{-8} and k_q is the quenching constant. Scatchard equation (vi) gives the binding properties of the complexes.[8] Where K = binding constant and n = number of binding sites.

$$\log(I_0 - I/I) = \log K + n\log[Q] \quad (vi)$$

Same procedure has been followed for HSA interaction study with these complexes.

Conductivity measurement

To substantiate the interaction of these complexes with water, DMSO, GSH and ct-DNA solutions, conductivity of the prepared complexes were measured using conductivity-TDS meter-307 (Systronics, India) and cell constant 1.0 cm^{-1}.[9] Rate of conductivity was also measured in different pH medium. Time dependent Conductivity measurement was also performed. The results are also compared with Cisplatin.

n-Octanol–buffer partition coefficient (log $P_{o/w}$)

The n-Octanol–buffer partition coefficient (log $P_{o/w}$) of the synthesized complexes was determined by means of shake flask method following the previously published procedure.[10] A known amount of each complex was suspended in PBS buffer in presence of 130 mM NaCl at PH 7.4 (pre-saturated with n-octanol) and shaken for 48 h on an orbital shaker. To allow the phase separation, the solution was centrifuged for 10 min at 3000 rpm. After the separation of two layers, they were subjected to UV-Vis spectroscopic analysis. Then the partition coefficient (log $P_{o/w}$) values were calculated using the OD of the complex in buffer and octanol medium.

References:

1. P. Liu, B. Wu, J. Liu, Y. Dai, Y. Wang, K. Wang, DNA Binding and Photocleavage Properties, Cellular Uptake and Localization, and in-Vitro Cytotoxicity of

Dinuclear Ruthenium(II) Complexes with Varying Lengths in Bridging Alkyl Linkers, *Inorg. Chem.* 2016, **55**, 1412−1422.

2. K. Purkait, S. Chatterjee, S. Karmakar and A. Mukherjee, Alteration of steric hindrance modulates glutathione resistance and cytotoxicity of three structurally related RuII-*p*-cymene complexes, *Dalton Trans.*, 2016, **45**, 8541-8555.
3. M. Sirajuddin, S. Ali, A. Badshah, Drug–DNA interactions and their study by UV–Visible, fluorescence spectroscopies and cyclic voltammetry, *J. Photochem. Photobio. B*., 2013, **124**, 1–19.
4. M. Shamsi-Sani, F. hirini, SM. Abedini, M. Seddighi, Synthesis of benzimidazole and quinoxaline derivatives using reusable sulfonated rice husk ash (RHA-SO3H) as a green and efficient solid acid catalyst, *Res. Chem. Intermed*., 2016, **42**, 1091–1099.
5. S. Dasari, A. K. Patra, Luminescent europium and terbium complexes of dipyridoquinoxaline and dipyridophenazine ligands as photosensitizing antennae: structures and biological perspectives, *Dalton Trans*., 2015, **44**, 19844-19855.
6. J. Keizer, Nonlinear fluorescence quenching and the origin of positive curvature in Stern-Volmer plots, *J. Am. Chem. Soc*., 1983, **105**, 1494–1498.
7. V. D. Suryawanshi, L. S. Walekar, A. H. Gore, P. V. Anbhule, G. B. Kolekar, Spectroscopic analysis on the binding interaction of biologically active pyrimidine derivative with bovine serum albumin, *J. Pharm. Anal*., 2016, **6**, 56–63.
8. K. Jeyalakshmi, J. Haribabu, C. Balachandran, S. Swaminathan, N. S. P. Bhuvanesh, R. Karvembu, Coordination Behavior of N,N′,N″-Trisubstituted Guanidine Ligands in Their Ru–Arene Complexes: Synthetic, DNA/Protein Binding, and Cytotoxic Studies, *Organometallics,* 2019, **38**, 753−770.
9. S. Nikolić, L. Rangasamy, N. Gligorijević, S. Aranđelović, S. Radulović, G. Gasser, S. Grgurić-Šipka, Synthesis, characterization and biological evaluation of novel Ru(II)–arene complexes containing intercalating ligands, *J. Inorg. Biochem.,* 2016, **160**, 156–165.
10. M. Kubanik, H. Holtkamp, T. Söhnel, S. M. F. Jamieson, C. G. Hartinger, Impact of the Halogen Substitution Pattern on the Biological Activity of

Organoruthenium 8-Hydroxyquinoline Anticancer Agents, *Organometallics*, 2015, **34**, 5658–5668.